not appear to be the case that loss of transcortical input to a region per se causes focal slow waves (although there may be a focal increase in coherence). An exception here concerns the hippocampus. Data from epileptic patients with hippocampal atrophy and sclerosis,[31] and also data from Alzheimer's patients with hippocampal atrophy,[32] converge to indicate that hippocampal damage often gives rise to focal slow waves in the temporal neocortex, especially anterior temporal projection zones. In this study, many patients with memory problems showed temporal slow waves. To some extent, this may reflect primary pathophysiology of the temporal neocortex, but in most cases, it probably reflects underlying damage to the hippocampus, as has been noted in several other studies showing disruption of hippocampal integrity following mild HT.[12,28]

Validity and specificity of findings

It must be remembered that there is presently no "gold standard" for the identification of traumatic brain injury in cases of mild HT. All that is certain is that each of our patients experienced a witnessed mild HT, and each reported some persistent problem.

A noteworthy observation from this study is that structural (MRI), hemodynamic (SPECT), and electrophysiological (MEG) methods all failed to provide results that correlated significantly with the presence of postconcussive psychiatric symptoms. This suggests that such symptoms may not directly reflect TBI, but rather may be secondary psychological reactions to other posttraumatic factors. Some of these other factors may directly reflect TBI (eg, changes in cognitive status as discussed below), while others do not (eg, social and economic consequences).

Considering somatic symptoms, there was a statistically significant relation between basal ganglia hypoperfusion and persistent headaches. Admittedly, the number of participants who showed both basal ganglia hypoperfusion and headaches was small ($N = 5$), but the statistical tests used take into account the data from all 30 participants and consider all combinations of being positive versus negative for basal ganglia findings and positive versus negative for headaches. While the present study did not have a normal comparison group, a review of the literature suggests that the false positive rate for identifying SPECT abnormalities in normal participants is less than 5%. It is also noteworthy that SPECT failed to demonstrate basal ganglia abnormalities in patients with mild HT reporting cognitive or psychiatric symptoms without headache (but, see reference 17, for contrary data). This suggests that there is specificity for this basal ganglia observation, although the extent to which subcortical hypoperfusion is seen in patients with headaches without head trauma is not known at present.

Although not especially sensitive to psychiatric or somatic complaints, MEG was highly likely to be abnormal when cognition was disturbed. For the 22 patients with cognitive complaints, MEG was abnormal for 18. Assuming that some of the patients in this study were malingering (all had passed malingering tests during neuropsychological evaluation), this observation, coupled with the significant relations between specific cognitive findings and region-specific MEG findings, suggests that MEG may serve as a neuroimaging gold standard for identifying TBI in patients with persistent postconcussive complaints subsequent to mild HT.

However, with respect to the relations between MEG findings and cognitive problems, the study is limited by a lack of baseline (pretrauma) cognitive data for the subjects. This issue is further compounded by the fact that neuropsychological deficits following mild HT are often subtle. For this study, we considered a domain to be abnormal if performance on relevant tests was at least 1 SD below the mean and the participant indicated he or she was impaired in that domain, the latter criterion being an attempt to gauge the perceived impact of subtle deficits. Supporting the validity of this strategy is the observation that, whenever neuropsychological testing revealed a deficit greater than 1.5 SD below the mean, participants always self-reported a deficit in that domain. Across all participants, there were 5 data points of neuropsychological test performance 1.0–1.5 SD below the mean, but participants did not report problems in the implicated domain. In the main analyses, these data points were coded as within normal limits. A follow-up analysis with these points coded as abnormal (based solely on the neuropsychological testing criteria) did not alter the significance levels for any of the relations reported herein.

Our conclusions are also constrained by the fact that performance in a domain was typically assessed by only 1 or 2 specific tests, and in some cases, a given test may tap multiple domains of processing. This was especially true with respect to tests included in the evaluation of processing speed (Trails B and the grooved pegboard task). However, a reassessment of processing speed considering just data from Trails A (as the data from Trails A and the CPT) still revealed a significant relation between processing speed and MEG slow waves from the temporal lobes. Also, cognitive constructs beyond processing speed that are thought to be tapped by Trails B and the pegboard task are not ones that would bias the data toward finding a correlation with the temporal lobes.

The number of comparisons between regional imaging findings and specific symptoms raises some concern about type 1 errors. The relations between specific imaging findings and deficits in memory, attention, and executive function were each consistent with prior data in the SPECT and MEG literature, and were all significant at $P < .01$, so it is unlikely that they reflect a type I error. The relation between basal ganglia hypoperfusion and headache has not been reported previously and the number of cases with both findings is small, but the significance level was quite high ($P < .001$, OR = 55), so this, too, is unlikely to be a type I error. The relation between processing speed and temporal lobe slow waves is a bit more suspect since there are no supporting observations in the literature and the significance level was low ($P < .05$). However, even using a sequential correction procedure to correct for multiple comparisons, the finding remains significant.

Given the above factors, the observed relations between specific MEG findings and specific symptoms are likely to be valid. There are, however, important considerations on the specificity of MEG observations of focal slowing in relation to head trauma. The specificity depends, of course, on the nature of the comparison group. In previously published and unpublished analyses of more than 70 normal comparison participants, we have found focal slowing in fewer than 10%.[21,33] There is a slightly increased incidence of slowing in patients with mild HT without cognitive symptoms, but even here, focal slowing is seen in only 15%.[28] It is also clear that cognitive compromise (in the absence of head trauma) is not always associated with focal slowing. For example, in both children and adults with attention problems related to attention-deficit disorder, focal slowing is seen far fewer than 15% (J. D. Lewine, J. T. Davis, and M. E. Funke, in preparation). These observations, combined with the significance of the relations between specific MEG patterns and specific cognitive symptoms, support the view that our liberal criteria for postconcussive cognitive compromise (1 SD below the mean) are viable for this population.

Although focal slowing in MEG appears to be a sensitive and specific marker of pathophysiology in distinguishing patients with traumatic brain injury from normal control participants, trauma patients without cognitive compromise, and some patient groups with cognitive compromise in the absence of head trauma, there are several nontrauma populations where the rate of focal slowing is quite high (between 30% and 80%). Specifically, bipolar slow wave activity has been reported for patients with tumors,[34,35] chronic stroke,[36,37] epilepsy,[38,39] dementia,[40] and schizophrenia.[41] Thus, in the absence of previous data or solid evidence that none of the above conditions are present at the time of MEG, some caution must be exercised in attributing the presence of slow waves explicitly to a temporally remote head injury.

Resting versus activation studies

There is a growing trend in imaging science to employ activation tasks to explore the impact of disease at brain function. For example, in studies using PET, SPECT, fMRI, EEG, or MEG in the evaluation of patients with dementia, it is common to collect imaging data during performance of a recognition memory task.[42] While the activation approach has proven quite fruitful from a cognitive neuroscience perspective where there is great advantage in having behavior and imaging measures coupled in time, it has not been especially useful in the evaluation of single patients. First, for at least PET and SPECT, there is a significant confound between imaging results and the behavioral ability to perform a task. In many cases it is unclear whether reduced activation is a cause or consequence of behavioral compromise. Also, in general, there is high between-participant variability in activation results, so differences between patient populations and normal controls can often be seen only in group-averaged data. Finally, activation paradigms are generally designed to probe very specific cognitive functions mediated by a restricted set of neuronal structures. So, using an activation approach, it is difficult to probe the full imaging space unless one uses many tasks.

In contrast, studies of baseline resting activity allow one to look for dysfunction throughout the brain, without a priori assumptions about relations between specific tasks and regions of activation. Also, available data suggest that intrasubject variability in resting measures is surprisingly low, so it is relatively easy to identify normal activity versus abnormal activity using either subjective or objective (statistical) approaches. These are critical concerns in evaluation of patients with mild HT, especially because there are significant interindividual differences in symptom profiles. Nevertheless, in future studies, it may be of value to combine activation and resting strategies to give the most comprehensive view possible.

Limitations

In evaluating the present data, several limitations must be kept in mind. First, the study is retrospective rather than prospective in nature. Patients were clinically referred rather than directly recruited from a trauma care center, and only those reporting persistent postconcussive psychiatric, somatic, or cognitive symptoms were included. Thus, the abnormality rates reported above should not be taken to reflect the incidence of MRI, SPECT, or MEG abnormalities in an unselected population of mild HT survivors—most of whom will not show persistent symptoms or imaging abnormalities. It should also be noted that the extent to which functional imaging might reveal abnormalities in symptomatic whiplash patients was not addressed by the current data.

Approximately 50% of our patients were on regular dosages of psychoactive medications, and even though such medications were withheld on the days of functional imaging, given the fallible of most of these medications, they could have affected imaging findings. While this was not formally examined in this study, we have (at least with respect to MEG) explicitly examined medication effects in patients with major depression, obsessive-compulsive disorder, schizophrenia, and attention-deficit disorder. In no case have we found that the medications used by trauma patients here result in an increase in DSWA, although in schizophrenia, these medications can cause a reduction in slow waves (J. D. Lewine, unpublished observations, 2007).

It must also be remembered that the present study examined only long-term consequences of trauma. While objective evaluation of the long-term structural and functional consequences of head trauma is of mechanistic, clinical, and legal interest, future studies should evaluate patients soon after trauma, with a goal of predicting which patients will have persistent postconcussive syndromes.

Another qualification of the present study is the fact that data were interpreted in a routine clinical manner and not using more sophisticated quantitative and statistical strategies that might produce a higher yield for each imaging modality. For example, Bigler and colleagues have shown that quantitative tools for assessing ventricular dilation subsequent to head trauma lead to the identification of abnormalities in a greater percentage of participants than when MR data are simply visually inspected by a clinician.[26] It must also be noted that a number of additional MR imaging sequences (eg, diffusion weighted imaging,[43] magnetization transfer imaging[44]) and other functional methods (including PET,[26,34] fMRI,[14,20] magnetic resonance spectroscopy,[45] quantitative EEG,[21,28] and evoked potentials[21]) may be useful in the evaluation of mild HT.

Finally, while MEG appears to be a more sensitive than MRI and SPECT to TBI in patients with persistent cognitive symptoms subsequent to mild HT, MEG is not yet widely available, with fewer than 25 whole-head MEG systems in the United States and fewer than 150 systems installed worldwide. On the other hand, it is likely that the next 5 to 10 years will see MEG availability extended to most major metropolitan regions, so the clinical potential for this imaging modality in the evaluation of head trauma patients must not be ignored.

REFERENCES

1. Rosenthal M, Christensen BK, Ross TP, et al. Postconcussion disorder following traumatic brain injury. *J Head Trauma Rehabil*. 1998;13(4):1–17.
2. Rosenthal M, Christensen BK, Ross TP, et al. Postconcussion disorder following traumatic brain injury. *J Head Trauma Rehabil*. 1998;13(4):1–17.
3. Rosenthal M, Christensen BK, Ross TP, et al. Postconcussion disorder following traumatic brain injury. *J Head Trauma Rehabil*. 1998;13(4):1–17.
4. Rosenthal M, Christensen BK, Ross TP, et al. Postconcussion disorder following traumatic brain injury. *J Head Trauma Rehabil*. 1998;13(4):1–17.
5. Rosenthal M, Christensen BK, Ross TP, et al. Postconcussion disorder following traumatic brain injury. *J Head Trauma Rehabil*. 1998;13(4):1–17.
6. Rosenthal M, Christensen BK, Ross TP, et al. Postconcussion disorder following traumatic brain injury. *J Head Trauma Rehabil*. 1998;13(4):1–17.
7. Rosenthal M, Christensen BK, Ross TP, et al. Postconcussion disorder following traumatic brain injury. *J Head Trauma Rehabil*. 1998;13(4):1–17.
8. Rosenthal M, Christensen BK, Ross TP, et al. Postconcussion disorder following traumatic brain injury. *J Head Trauma Rehabil*. 1998;13(4):1–17.
9. Rosenthal M, Christensen BK, Ross TP, et al. Postconcussion disorder following traumatic brain injury. *J Head Trauma Rehabil*. 1998;13(4):1–17.
10. Rosenthal M, Christensen BK, Ross TP, et al. Postconcussion disorder following traumatic brain injury. *J Head Trauma Rehabil*. 1998;13(4):1–17.

25. Lewine JD, Davis JT, Sloan JH, et al. Neuromagnetic assessment of pathophysiological brain activity induced by minor head trauma. *Am J Neuroradiol*. 1999;20:857–866.
26. Bigler ED, Rosa L, Schultz F, et al. Quantitative magnetic resonance imaging and transcranial Doppler ultrasonography in moderate to severe traumatic brain injury. *J Neuropsychiatry Clin Neurosci*. 1997;9(2):133–136.
27. Bigler ED, Rosa L, Schultz F, et al. Quantitative magnetic resonance imaging and transcranial Doppler ultrasonography in moderate to severe traumatic brain injury. *J Neuropsychiatry Clin Neurosci*. 1997;9(2):133–136.
28. Bigler ED, Rosa L, Schultz F, et al. Quantitative magnetic resonance imaging and transcranial Doppler ultrasonography in moderate to severe traumatic brain injury. *J Neuropsychiatry Clin Neurosci*. 1997;9(2):133–136.
29. Bigler ED, Rosa L, Schultz F, et al. Quantitative magnetic resonance imaging and transcranial Doppler ultrasonography in moderate to severe traumatic brain injury. *J Neuropsychiatry Clin Neurosci*. 1997;9(2):133–136.
30. Bigler ED, Rosa L, Schultz F, et al. Quantitative magnetic resonance imaging and transcranial Doppler ultrasonography in moderate to severe traumatic brain injury. *J Neuropsychiatry Clin Neurosci*. 1997;9(2):133–136.
31. Bigler ED, Rosa L, Schultz F, et al. Quantitative magnetic resonance imaging and transcranial Doppler ultrasonography in moderate to severe traumatic brain injury. *J Neuropsychiatry Clin Neurosci*. 1997;9(2):133–136.
32. Bigler ED, Rosa L, Schultz F, et al. Quantitative magnetic resonance imaging and transcranial Doppler ultrasonography in moderate to severe traumatic brain injury. *J Neuropsychiatry Clin Neurosci*. 1997;9(2):133–136.
33. Bigler ED, Rosa L, Schultz F, et al. Quantitative magnetic resonance imaging and transcranial Doppler ultrasonography in moderate to severe traumatic brain injury. *J Neuropsychiatry Clin Neurosci*. 1997;9(2):133–136.
34. Bigler ED, Rosa L, Schultz F, et al. Quantitative magnetic resonance imaging and transcranial Doppler ultrasonography in moderate to severe traumatic brain injury. *J Neuropsychiatry Clin Neurosci*. 1997;9(2):133–136.
35. Bigler ED, Rosa L, Schultz F, et al. Quantitative magnetic resonance imaging and transcranial Doppler ultrasonography in moderate to severe traumatic brain injury. *J Neuropsychiatry Clin Neurosci*. 1997;9(2):133–136.
36. Bigler ED, Rosa L, Schultz F, et al. Quantitative magnetic resonance imaging and transcranial Doppler ultrasonography in moderate to severe traumatic brain injury. *J Neuropsychiatry Clin Neurosci*. 1997;9(2):133–136.
37. Bigler ED, Rosa L, Schultz F, et al. Quantitative magnetic resonance imaging and transcranial Doppler ultrasonography in moderate to severe traumatic brain injury. *J Neuropsychiatry Clin Neurosci*. 1997;9(2):133–136.
38. Bigler ED, Rosa L, Schultz F, et al. Quantitative magnetic resonance imaging and transcranial Doppler ultrasonography in moderate to severe traumatic brain injury. *J Neuropsychiatry Clin Neurosci*. 1997;9(2):133–136.
39. Bigler ED, Rosa L, Schultz F, et al. Quantitative magnetic resonance imaging and transcranial Doppler ultrasonography in moderate to severe traumatic brain injury. *J Neuropsychiatry Clin Neurosci*. 1997;9(2):133–136.
40. Bigler ED, Rosa L, Schultz F, et al. Quantitative magnetic resonance imaging and transcranial Doppler ultrasonography in moderate to severe traumatic brain injury. *J Neuropsychiatry Clin Neurosci*. 1997;9(2):133–136.
41. Bigler ED, Rosa L, Schultz F, et al. Quantitative magnetic resonance imaging and transcranial Doppler ultrasonography in moderate to severe traumatic brain injury. *J Neuropsychiatry Clin Neurosci*. 1997;9(2):133–136.
42. Bigler ED, Rosa L, Schultz F, et al. Quantitative magnetic resonance imaging and transcranial Doppler ultrasonography in moderate to severe traumatic brain injury. *J Neuropsychiatry Clin Neurosci*. 1997;9(2):133–136.
43. Bigler ED, Rosa L, Schultz F, et al. Quantitative magnetic resonance imaging and transcranial Doppler ultrasonography in moderate to severe traumatic brain injury. *J Neuropsychiatry Clin Neurosci*. 1997;9(2):133–136.
44. Bigler ED, Rosa L, Schultz F, et al. Quantitative magnetic resonance imaging and transcranial Doppler ultrasonography in moderate to severe traumatic brain injury. *J Neuropsychiatry Clin Neurosci*. 1997;9(2):133–136.
45. Bigler ED, Rosa L, Schultz F, et al. Quantitative magnetic resonance imaging and transcranial Doppler ultrasonography in moderate to severe traumatic brain injury. *J Neuropsychiatry Clin Neurosci*. 1997;9(2):133–136.

JOURNAL OF NEUROTRAUMA 29:654–671 (March 1, 2012)
© Mary Ann Liebert, Inc.
DOI: 10.1089/neu.2011.1908

Emerging Imaging Tools for Use with Traumatic Brain Injury Research

Jill V. Hunter,[1,2] Elisabeth A. Wilde,[3,4] Karen R. Tong,[5] and Barbara A. Holshouser[1]

Abstract

This article identifies emerging neuroimaging measures considered by the inter-agency Pediatric Traumatic Brain Injury (TBI) Neuroimaging Workgroup. This article attempts to address some of the potential uses of more advanced forms of imaging in TBI as well as highlight some of the current considerations and unresolved challenges of using them. We summarize emerging elements likely to gain more widespread use in the coming years, because of 1) their utility in diagnosis, prognosis, and understanding the natural course of degeneration or recovery following TBI, and potential for evaluating treatment strategies; 2) the ability of many centers to acquire these data with sciences and equipment that are readily available in existing clinical and research settings; and 3) advances in software that provide more automated, readily available and cost-effective analysis methods for large scale data image analysis. These include multi-slice CT, volumetric MRI analysis, susceptibility-weighted imaging (SWI), diffusion tensor imaging (DTI), magnetization transfer imaging (MTI), arterial spin tag labeling (ASL), functional MRI (fMRI), including resting state and connectivity MRI, MR spectroscopy (MRS), and hyperpolarization scanning. However, we also include brief introductions to other specialized forms of advanced imaging that currently do require specialized equipment, for example, single photon emission computed tomography (SPECT), positron emission tomography (PET), encephalography (EEG), and magnetoencephalography (MEG)/magnetic source imaging (MSI). Finally, we identify some of the challenges that users of the emerging imaging CDEs may wish to consider, including quality control, performing multi-site and longitudinal imaging studies, and MR scanning in infants and children.

Key words: adults; children; CT; MRI; neuroimaging; TBI

Introduction

The Common Data Elements (CDE) initiative for traumatic brain injury (TBI) is an attempt to promote integration in measures applied in TBI research. As previously reported, the original TBI CDE recommendations were formulated using three descriptive levels: "core" elements that are intended to encompass a minimal set of measures to characterize a broad spectrum of subjects; "supplemental" elements that are intended for greater depth or breadth of exploration or are intended for more specialized subpopulations; and "emerging" elements that represent measures with significant potential to expand knowledge in the field, but that currently require further validation or special consideration (Thurmond et al., 2010).

Emerging neuroimaging tools with the potential to inform TBI research have been previously identified, both by the original Neuroimaging Workgroup (Duhaime et al., 2010; Hacke et al. 2010) and the Pediatric Neuroimaging Workgroup (Duhaime, 2011). The recommendations for core and supplemental CDEs from the original Neuroimaging Workgroup were generally focused on conventional imaging, largely because of the need to establish radiological definitions for terms of injury identifiable on conventional imaging sequences, and also because these techniques are widely available in many TBI-related studies and across centers. However, the group acknowledged that a number of more advanced imaging modalities exists and have great potential to further our understanding of TBI. Although the group did specify some specific techniques and suggested parameters for optimal acquisition in some imaging techniques (see Appendix B of Hacke et al., 2010 or http://www.commondataelements.ninds.gov), both the original and pediatric workgroups acknowledged that prescription of specific protocols for

[1]Department of Pediatric Radiology, Texas Children's Hospital, Houston, Texas.
[2]Departments of Radiology and [3]Physical Medicine, Rehabilitation, and Neurology, Baylor College of Medicine, Houston, Texas.
[4]Michael E. DeBakey Veterans' Administration Medical Center, Houston, Texas.
[5]Department of Radiology, Loma Linda University School of Medicine, Loma Linda, California.

were of the advanced modalities was problematic and required further considerations, as these forms of imaging are still evolving, require further validation or standardization, and continue to pose challenges for use across different groups of investigators.

This article attempts to provide additional detail regarding some of the potential uses of more advanced forms of imaging, in TBI as well as highlight some of the current considerations and unresolved challenges of each. It is intended for investigators who wish to consider applying advanced neuroimaging techniques in TBI-related studies. Although this article accompanies other recommendations for CDEs in pediatric TBI research, and places an emphasis on issues that may be important in early development, the following comments generally apply to the use of basic modalities in adults as well as infants, children and adolescents.

Selection of Emerging Imaging Measures

Neuroimaging is a rapidly evolving field, and the potentially useful techniques discussed in this article are by no means exhaustive. Nor are modalities that are already in use in TBI research. Additionally, other forms of structural and functional imaging will also be developed or come into use in the near future as technology advances. However, we have attempted to summarize emerging elements that are most likely to gain more widespread use in the coming years, because of 1) their utility in diagnosis, prognosis, and understanding the natural course of degeneration or recovery following TBI, and potential for evaluating treatment strategies; 2) the ability of many centers to acquire these data with sciences and equipment that are readily available in existing clinical and research settings; and 3) advances in software that provide more automated, readily available, and cost-effective analysis methods for large scale data image analysis. We also include a brief introduction to a couple of new or more-specialized forms of advanced imaging that do require specialized equipment or software, for example, positron emission tomography (PET) and magnetoencephalography (MEG)/magnetic source imaging (MSI). Finally, we identify some of the general and unique challenges that users of the emerging imaging CDEs may wish to consider. The emerging neuroimaging tools commented upon in this article include:

- multi-slice CT
- volumetric MRI analysis
- susceptibility-weighted imaging (SWI)
- diffusion tensor imaging (DTI)
- magnetization transfer imaging (MTI)
- arterial spin tag labeling (ASL)
- functional MRI (fMRI), including resting state and connectivity MRI
- MR spectroscopy (MRS)
- PET and single photon emission computed tomography (SPECT)
- MSI or MEG
- hyperpolarization scanning

Several excellent reviews of the use of some of these techniques in TBI have been previously published, and may provide additional information (Ashwal et al., 2006a; Belanger et al., 2007; Cullen, 2007; Gallagher et al., 2007; Hillary et al., 2010; Kou et al., 2010; Sankaran and Huisman, 2009; Tshibanda et al., 2009; Van Boven et al., 2009). As with all the CDE recommendations, the selection of recommended outcome measures is an evolving process and recommendations may change with additional evidence and ongoing discussions regarding the current CDEs. Therefore, the Workgroup advises the reader to consult the CDE website (http://www.commondataelements.ninds.gov) for any updates and information, particularly with respect to these emerging measures.

General Considerations in the Use of Emerging Imaging Measures

Quality control

Particularly for the advanced imaging MRI sequences, quality assurance (QA) testing is essential for ensuring the fidelity of the data acquired. Scanners should undergo qualification prior to the beginning of subject enrollment and be re-qualified following hardware or software upgrades, using a specific QA protocol (Friedman and Glover, 2006; Friedman et al., 2006) and a specific phantom to ensure optimal scanner performance (Van Boven et al., 2009). For example, in other large collaborative groups that have endeavored to use multi-site imaging, such as the Alzheimer's Disease Neuroimaging Initiative (ADNI), a phantom scan is acquired with each subject, allowing identification of scanning errors or correction of drifts or discontinuities in the decrypted human data. Frequent (weekly or more often) repeated QA with designated phantoms, for example, General Electric (GE), Biomedical Informatics Research Network (BIRN), gel or "doped" water bottle for Siemens) testing (Weisskoff, 1996), or use of a "travelling" human phantom (i.e., the same individual is scanned on each of the different scanners) for multi-site studies is strongly recommended.

Once acquired for during acquisition, all data should be reviewed for compliance with the protocol. Image quality, presence of any significant artifact that would compromise accuracy or reliability (including, where applicable, motion, susceptibility, eddy current, dental or metal artifact) and incidental or medically significant findings that would impact study inclusion or exclusion criteria, should all be assessed. Additional post-processing correction specific to each modality should then be applied in a uniform manner (preferably by a single center) to correct for issues such as gradient nonlinearity, intensity inhomogeneity, motion, or eddy current.

Multi-center studies

Several obstacles have prevented more widespread use of the advanced MRI modalities. The first of these is the broad range of hardware and software platforms that exist across different sites. Differences related to the scanner manufacturer (e.g., General Electric vs. Philips vs. Siemens) may introduce significant unwanted variability in the data, as each approaches the acquisition and standard parameters somewhat uniquely, leading to differences in contrast (important for volumetrics), regions prone to artifact or distortion (especially important to echo planar imaging sequences for DTI and fMRI), and level of noise. Establishing equivalency in sequences and parameters across different scanner manufacturers remains extremely challenging. Even when scanners of the same manufacturer are used, differences in the scanner model should be carefully considered, as this may also introduce

variability in the data that are acquired. Site-specific issues including radio frequency (RF) shielding and vibration will also vary from one location to another. Field strength (e.g., 1.5 Tesla vs. 3 Tesla) may also introduce differences in data secondary to signal-to-noise ratio (SNR) and degree of resolution. Next, head coil differences may introduce variability (e.g., 8-channel vs. 16-channel vs. 32-channel). Finally, differences in scanner software release may alter quantitative measurement in imaging data, and this remains a challenge in most major medical centers where upgrades can occur frequently. Ideally, for very sensitive modalities such as diffusion tensor imaging, multi-site centers should use the same scanner manufacturer, scanner model, software release, head coil, field strength, and acquisition parameters, where possible, although this clearly limits the number of sites that can be included, and becomes problematic for clinical trials and large-scale studies. Alternatively, general comparability of data acquired at different sites should be demonstrated before data are pooled. Although there has been some discussion among members in the field related to creation of "standard scans" derived from actual values in modalities such as DTI, MRS, and MTI to address this issue, no optimal solution has yet been established. Additional obstacles have historically included significant variability in levels of expertise, experience, and access to equipment and software for comparable data post-processing and analysis.

Longitudinal studies

Perhaps the most significant challenge in the use of advanced imaging modalities in longitudinal research is simply the rapid pace at which technology evolves in this area. Within the life of a project sufficiently long enough to collect an adequate amount of longitudinal data, acquisition parameters (e.g., the number of gradient directions in DTI) or analysis methodology or software versions initially established at the outset may be considered "outdated" by the completion of a longer study (e.g., new software releases frequently available programs may occur yearly or even more often). As previously mentioned, scanner software upgrades also occur as technology advances, and the impact of these upgrades on certain advanced MRI sequences may be inevitable in longitudinal studies in which quantitative data analyses are involved. Therefore, longitudinal studies require careful consideration of these factors, and some formal testing and monitoring of the impact of these factors may be required throughout the study. In the case of upgrades in analysis software, comparison of analyses using subsets of data analyzed on each version may be advisable to ensure comparability in results. Obtaining pre- and post-scanner upgrade data on a limited number of subjects may be done to determine (and potentially adjust for) any impact of the upgrade.

Modality-specific challenges also exist in the analysis of longitudinal data, particularly for region-of-interest (ROI) approach techniques in structural imaging, where exact replication in placement of an ROI is difficult either because of changes in the placement of the slices or degenerative change that necessitates elimination in the use or placement of the ROI. The reproducibility of some advanced techniques, particularly in regard to functional imaging modalities, also deserves careful consideration.

Finally, the analysis of longitudinal data, especially in infants, children, and adolescents, requires careful consideration of the underlying developmental context and how TBI-related sequelae may interact with developmental changes that are co-occurring over time. Expected developmental trajectories may differ by age, gender, handedness, region of the brain, and tissue type, and some imaging modalities may be more impacted by developmental changes than others, and the direction of this change may alter by modality.

Scanning in children

Because of the increased speed of acquisition with modern CT scanners, most children do not require sedation for imaging of the brain on unenhanced CT. However, acquisition of lengthy sequences in MRI can present challenges because of the increased potential for motion artifact, particularly in children with acute or severe injury or in children with TBI-related attentional difficulties or impulsivity. Motion during imaging may be mitigated to some degree by mock scanner training and repeated instruction to the child to remain still. Normally developing children, and even those with TBI, >8 years of age can typically be accommodated in the MR scanner without sedation. High functioning children <8 years of age may also be able to remain still in the scanner (often with a parent present in the scanner room). Some 1 Tesla scanners are physically quieter than conventional 1.5 Tesla instruments and may create more difficulty for the younger child to lie still. Although many institutional review boards will not approve protocols requiring sedation for the purpose of research, most conventional examinations can be acquired without data alterations with conscious sedation. However, it is recognized that certain anesthetic agents (e.g., propofol) may alter and decrease the activation seen with functional imaging paradigms. Moreover, functional imaging modalities (fMRI and MSI) may require increased monitoring of levels of alertness in children.

Description of Emerging Imaging Techniques and Unique Considerations

CT

CT scanning continues to form the mainstay for clinical screening of TBI, because of its speed and reproducibility in allowing identification of fresh blood and some acute parenchymal injury, in addition to giving information regarding the presence of bony injury in both the head and spine. However, early CT scanning immediately following injury may miss later development of hemorrhagic shear injury and enlargement of extra-axial collections, which are both typically apparent by 24 h post-TBI.

In recent years, multi-detector technology has been introduced that permits 4-sec scan times of the brain with a 64-slice scanner. This very fast scan time and near-zero patient/scanner-related scans to be performed without sedation. Recent introduction of a 320-row detector CT scanner holds the promise of even faster acquisition times (1–2 sec), and scans may be performed in either axial or helical mode, the latter being a volumetric examination. This latest technology is still being assessed in the field to ensure that radiation dosage for soft tissues such as the brain can be maintained at a low level without compromising the detection of pathology because of a reduction in signal to noise. The guiding principle is acquisition at the lowest acceptable radiation dose (ALARA). Helpful guidelines for clinicians and parents regarding reductions in radiation dosage may be found at www.imagegently.com. Because of the concern surrounding CT-related ionizing radiation exposure, particularly in children, use of CT solely as a research tool is not advised. However, clinically indicated CT results are often used in TBI research for characterization of the patient cohort(s), description of the size and nature of acute lesions or abnormalities, determination of participant eligibility (e.g., treating inclusion or exclusion criteria), or for injury severity stratification purposes.

MRI

Conventional MRI imaging including T1-weighted, T2-weighted and T2 fluid-attenuated inversion recovery (FLAIR) sequences as well as T2* (gradient echo) and diffusion-weighted imaging (DWI) are used in routine clinical practice for patients with TBI. They may give some important information concerning visible hemorrhage and extra-axial collections as well as demonstration of early ischemia and possible detection of edema in sub-acute moderate-to-severe injury. However, detection of abnormalities in uncomplicated early acute mild TBI (as determined by normal CT) with conventional sequences is uncommon in the authors' experience and more moderate-to-severe brain-injured subjects may be too unstable to undergo MRI scanning readily.

Volumetric analysis. Volumetric analysis allows for the detection or quantification of white and gray matter volumes, either globally or for specific regions, as well as cerebrospinal fluid and total intracranial volume, generally using three-dimensional (3-D) volumetric high resolution T1-weighted imaging or combinations of complementary MR sequences. Volumetric analysis using such techniques has demonstrated significant decreases in volume in both adult (Tzoumaka et al., 2004; Warner et al., 2010a; Wilde et al., 2004, 2006a) and pediatric (Beauchamp et al., 2008, 2010; Bonfiglio et al., 2008; Spanos et al., 2007; Wilde et al., 2005, 2006b, 2007; Wu et al., 2010b) subjects with TBI in the chronic post-injury interval. Additionally, voxel-based, whole-surface based, and lobar-based analyses have also demonstrated significant global reductions in cortical thickness (Merkley et al., 2008) and cortical gray matter volume (Bigler et al., 2010a, Ding et al., 2008; Lee et al., 2005; Warner et al., 2010a,b) as well as white matter volume (Ding, 2009; Levine et al., 2008; Sidaros et al., 2009; Yanasoldati et al., 2010). Late volumetric measures have demonstrated relation to measures of clinical severity (Levine et al., 2008; Schimberger et al., 2009; Trivedi et al., 2007), outcome, (Ding et al., 2008; Gale and Pogatzki, 2010; Warner et al., 2010b), cognition (Bergeson et al., 2004; Fujiwara et al., 2008; Hanaway et al., 2005; Sena-Gesbalosa et al., 2005; Tomaszewski et al., 2005; Warner et al., 2010a), and potential for benefit from rehabilitation intervention (Strangman et al., 2010), although other studies have reported no correlation between volumetric measures and functional outcome (Andreason et al., 1995; Sharer et al., 2006; Yount et al., 2002).

Whereas volumetric analysis is an emerging neuroimaging tool and has been successfully used in large-scale analyses of data acquired using different scanners and protocols such as those performed by the Alzheimer's Disease Neuroimaging Initiative (Chen et al., 2010; Hua et al., 2010; Mueller et al., 2005; Risacher et al., 2010; Simmons et al., 2011), challenges remain in its use in multisite studies in TBI. First, volumetric changes can evolve over an extended time (Sidaros et al., 2009; Trivedi et al., 2007; Wu et al., 2010a) and may be evident late than changes seen on other advanced imaging techniques such as DTI (Bendlin et al., 2008; Green et al., 2010; Huisman et al., 2010; Wu et al., 2010a). It should be kept in mind that the relation between tissue integrity, as measured by volumetry, and outcome may be dynamic and complex, particularly in the earlier phases of recovery, as trajectories of rapid cognitive recovery and incomplete degenerative tissue change may be progressing in opposing directions and to differing degrees. This relation becomes even more complex in infants, children, adolescents, and the elderly in whom TBI-related parenchymal and cognitive changes are occurring within a context of known developmental (or degenerative) brain changes (e.g., linear increase/decrease in white matter with myelination, regional reductions in regional cortical thickness and volume related to programmed apoptosis). Variability in severity of injury, nature and location of brain insult, mechanism of injury, and other co-morbidities present additional challenges for volumetric analysis in TBI. Semi-automated programs for volumetric measurement have emerged in recent years, several of which are freely available (e.g., FreeSurfer, FSL, SPMS), facilitating the potential for large-scale analyses using volumetric data. With the rapid evolution of technology in this area, both the accuracy of the results and the automation are increasing. Additionally, such programs allow for combination of volumetric data with data from other imaging modalities. However, such programs may still have some accuracy limitations in regions of the brain that are difficult to model (e.g., medial temporal areas) or that contain very large lesions or types of pathology (e.g., acute hemorrhage) that the software cannot accurately distinguish. The more automated methods of volumetric analysis generally only take into account a T1-weighted image; therefore, smaller lesions or certain kinds of pathology such as gliosis can be easily missed. Also, because of the dynamic changes that occur during infancy and early childhood in white matter secondary to myelination and the manner in which these are manifest on imaging (e.g., non-uniform signal intensity), many manual and semi-automated techniques suffer inaccuracies in segmentation of white and gray matter in very young children. Finally, determination of TBI-related cortical change requires an appropriate normative comparison, given the dynamic developmental changes that occur throughout the life span and potential differences related to gender and handedness.

SWI. SWI is a modified high spatial resolution 3D gradient recalled-echo (GRE) MR technique that accentuates the magnetic properties of blood products, thereby rendering it useful in detecting small amounts of chronic blood blood product on neuroimaging (Hatcher et al., 2004; Reichenbach et al., 1997; Sehgal et al., 2005). SWI has primarily been considered to be helpful in the identification of hemorrhagic axonal injury where smaller hemorrhages not visible on CT or conventional MRI sequences may be visualized with this technique (Ashwal et al., 2006b). SWI may be helpful in the detection of these "microhemorrhages," especially in early acute and sub-acute phases of injury, and in detecting areas of hypoxia-ischemia induced secondary injury. Figure 1 demonstrates the increased visibility of small hemorrhagic

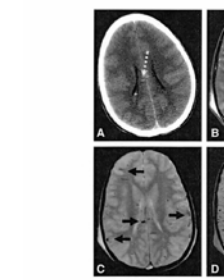

FIG. 1. CT (A) only shows a few small hyperdense hemorrhages in the corpus callosum (dashed white arrow) of a child with TBI. T2WI (B) is not sensitive to hemorrhage, although ill-defined T2 hyperintense areas of edema are detected in the corpus callosum and the periphery of the hemispheres (double line (black arrows). Conventional T2*-WI (C) is routinely used to detect hemorrhage, which demonstrates small hypointense hemorrhagic contusions along the brain surface as well as hemorrhagic shearing injury in the corpus callosum (solid black arrows). However, susceptibility-weighted imaging (SWI) (D) is significantly more sensitive to hemorrhage, and shows many more hemorrhages (white arrows) than any of the other images.

abnormalities demonstrated in SWI as opposed to other more conventional imaging modalities.

SWI has demonstrated increased sensitivity to the number and volume of hemorrhagic traumatic axonal injury lesions as compared to conventional T2*-weighted two-dimensional (2D)-GRE imaging (Tong et al., 2003), and the extent of SWI-identified hemorrhage has been shown to correlate with initial severity of injury (measured by Glasgow Coma Scale (GCS), duration of coma, long-term outcome measured at 6–12 months after injury (Tong et al., 2004), and specific neuropsychological deficits (Ashwal et al., 2006b). SWI is able to detect a larger number of lesions and to define smaller areas of damage than CT, T2-weighted imaging, and FLAIR imaging. However, SWI has not yet been shown to be superior to T2-weighted imaging or FLAIR in discriminating between good and poor outcomes (Chastain et al., 2009). There are currently conflicting results on the relationship between outcome and the number of lesions on MRI, given the few comparison studies available. Some studies report that lesions on T2WI (Chastain et al., 2009; Gerber et al., 2004; Sigmund et al., 2007), FLAIR (Chastain et al., 2009; Sigmund et al., 2007), T2*-GRE (Gerber et al., 2004; Yanagawa et al., 2000), and SWI (Sigmund et al., 2007; Tong et al., 2004), can discriminate or correlate with outcomes. Other studies report that there is no correlation between outcomes and lesions on T2WI (Yanagawa et al., 2000), T2*-GRE (Scheid et al., 2003), and SWI (Chastain et al., 2009). It is likely that a combination of imaging findings will improve the ability to predict clinical outcome, and more studies are needed to confirm this.

In secondary injuries, SWI may also demonstrate increased oxygen extraction in areas of tissue infarction or hypoxemia. Increased deep medullary veins can be observed surrounding an area of infarction, which may reflect impaired cerebral blood flow (CBF) in the penumbra areound an infarct. In this zone, lower levels of oxygenated red blood cells, and therefore higher levels of deoxygenated red blood cells, may account for increased visibility of veins in these regions. In more severe global hypoxic injury, increased oxygen extraction may reflect catastrophic brain insults in those children who become brain dead. The evolution of injury after severe hypoxia-ischemia includes a period of time when increased oxygen extraction occurs as CBF dramatically decreases because of increasing cerebral edema and increased intracranial pressure (ICP).

A detailed explanation of the underlying physics and mathematical principles is described in depth in several recent publications (Haacke et al., 2004; Sehgal et al., 2005) and parameters for the original and modified sequences have been previously published. The sequence along with its automatic post-processing is currently available for Siemens 1.5 and 3.0 Tesla MRI scanner platforms, as well as on other recent scanner platforms from Toshiba and Philips. GE has a different version, known as SWAN (T2 Star Weighted Angiography), without the extensive post-processing. In the future, it is likely that this method, particularly a faster version, will replace conventional T2*-GRE imaging in clinical evaluation as well as research studies. Remaining challenges in using SWI in TBI research include its susceptibility to artifacts in air-tissue interfaces, including the orbital frontal areas, a regional deficit vulnerability in TBI. Adequate training and familiarity with the technique are needed to differentiate veins from small hemorrhages. In regards to the use of SWI in the detection of hemorrhage, SWI may not be as sensitive to subarachnoid hemorrhage in cisterns where bone structures are in dose proximity (Wu et al., 2010b). It is currently unknown whether SWI can be used to differentiate subarachnoid or subdural hemorrhage along the tentorium (Wu et al., 2010b).

DTI. DTI allows a potentially useful in vivo estimation of the integrity of white matter, as changes in diffusion or anisotropy measured by DTI are thought to be associated with microstructural alteration resulting from loss or disorganization of fibers associated with breakdown of myelin and axonal membranes, neuronal swelling or disorganization, and increased or decreased extracellular space (Ducreux et al., 2005). DTI allows measurement of the directionality of anisotropic diffusion (restricted diffusion is one direction with enhanced direction in another) of water molecules within coherently organized white matter tracts. The speed and direction of this diffusion renders information about the microstructural environment of the brain. Diffusion anisotropy can be quantified within white matter tracts using the DTI-derived measure fractional anisotropy (FA) or other DTI-derived diffusion metrics such as apparent diffusion

coefficient (ADC) or mean diffusivity (MD) or axial diffusivity (AD) or radial diffusivity (RD). Currently, this technique is considered to be most useful in the evaluation of axonal injury in white matter, although it has also been used to examine the microstructural properties of gray matter in TBI (Newsombe et al., 2006). Other advanced forms of DTI including diffusion spectrum imaging (DSI), high angular resolution diffusion imaging (HARDI), and q-ball are also demonstrating great promise and can resolve some of the known pitfalls of DTI for regions with crossing fibers, although these may require longer acquisition times and specific hardware requirements. Studies of TBI using DTI, as well as the software to analyze these data, have been steadily increasing in recent years. Significant differences in the FA, ADC, or MD, or other DTI-derived diffusivity metrics have been demonstrated in studies of TBI in both adults (Bigler et al., 2010b; Kraus et al., 2007; Lipton et al., 2008; Perlbarg et al., 2009; Warner et al., 2010a) and children (Ewing-Cobbs et al., 2008; Levin et al., 2008; McCauley et al., 2011; Wilde et al., 2008b, 2010; Wozniak et al., 2007; Wu et al., 2010a; Yuan et al., 2007), with decreases in FA and increases in measures of diffusivity often found in chronic post-injury intervals. More importantly, changes in DTI-derived measures have shown correlation with injury severity (Arfanakis et al., 2002; Benson et al., 2007; Wilde et al., 2010; Yuen et al., 2007), functional outcome (Ristanen et al., 2004; Levin et al., 2008; Salmond et al., 2006; Wozniak et al., 2007), neurologic functioning (Caeyenberghs et al., 2010a,b), and cognitive ability (Bigler et al., 2010b; Ewing-Cobbs et al., 2008; Kraus et al., 2007; Kumar et al., 2009; Levin et al., 2008; McCauley et al., 2011; Niogi et al., 2008; Salmond et al., 2006; Warner et al., 2010a; Wilde et al., 2010). Longitudinal studies have also indicated that DTI might serve as a tool for revealing changes in the neural tissue during recovery from TBI (Bendlin et al., 2008; Sidaros et al., 2009; Trivedi et al., 2007). DTI remains a promising tool in TBI research and clinical practice for 1) assisting in clinical diagnosis (particularly in mild TBI) (Huisman et al., 2010; Mayer et al., 2010; Niogi et al., 2008; Wilde et al., 2008) and prognosis (Newsombe et al., 2007; Perlbarg et al., 2009); 2) understanding the nature and time course of degenerative brain changes in vivo; 3) assessing potential evidence for neuroplastic changes (reorganization or recovery); and 4) evaluating therapeutic interventions and rehabilitation. It should be kept in mind that further studies will be necessary to validate and more completely understand the neurobiological basis that underlie differences in DTI-derived metrics (Adams et al., 2011), particularly given the complexity of TBI-induced tissue changes. Additionally, particular challenges surround the potential for its use in large-scale, multi-site, or longitudinal studies. Perhaps most significantly, it is difficult to establish the equivalency of quantitative measures derived from protocols that use different acquisition parameters (including but not limited to number of gradient directions, b-value, voxel size), scanner manufacturer and/or software platform, and field strength, or head coil. At this time, caution is advised in combining data collected from different sites or using different protocols. Second, DTI data can also be quite vulnerable to distortion and artifacts (i.e., metal, eddy current, motion, susceptibility), and there is no widely used threshold for determining "acceptable" data quality. Third, there is no consensus on which DTI metric (e.g., FA, ADC/MD, AD, RD) is best used in TBI-related studies, as each may be sensitive to different forms of pathology co-occurring in TBI. Indeed, studies using multiple metrics examining the relation of DTI to outcome have often found disparate results among the metrics. Fourth, certain forms of analysis, such as a single-slice ROI approach are difficult to use in longitudinal studies because the placement of the slices between the studies will inevitably vary, leading to further difficulty in the placement of an identical ROI. Fifth, in TBI, inclusion of subjects with large focal lesions may also cause challenges in many forms of analysis, particularly given field susceptibility from hemosiderin deposition, gliosis, and encephalomalacia which may alter diffusion parameters. Sixth, the time course of DTI-related changes remains unknown and may vary with injury severity, mechanism of injury, and age of the participants; therefore, these factors may require careful consideration. Finally, as with many advanced techniques, appropriate normative data are required because age-related differences can be substantial, particularly at the extremes of age. Given the sensitivity of DTI data to changes in just about any parameter, such normative data are ideally acquired on the same scanner using the same protocol.

Currently there are numerous commercially and freely available software packages for the processing and analysis of DTI data, and several different analysis methods exist, including (but not limited to) single- or multiple-slice ROI approaches, quantitative tractography, tract-based spatial statistics, voxel-based analysis, and histogram analyses. Each of these forms of analysis has advantages and disadvantages depending upon the question being addressed. A detailed listing of the limitations of each analytic technique is beyond the scope of this review, but researchers should be advised that differences in post-processing and analytic methods may produce differences in the results obtained.

MTI. MTI is a technique that uses an off-resonance saturation selective pulse to saturate protons associated with macromolecules. MT generates contrast based upon subtle molecular exchange processes in tissues. More specifically, the interaction between free water protons and macromolecular protons such as proteins and phospholipids, which exist the axonal membranes and myelin sheaths (Duckworth and Stevens, 2010) in the brain's microstructure. This exchange is achieved through magnetization interaction based on dipolar or chemical exchange (sometimes both). In order to do this, an off-resonance RF pulse is applied to macromolecular protons, and some of this excited magnetization is transferred to free water protons. The amount of this exchange can be quantified by calculation of the magnetization transfer ratio (MTR) (Wolff and Balaban, 1989). Exogenous contrast components are the major contributors to the MT effect in brain tissue, and therefore the concentration and integrity of myelin is reflected in MTR values (Dousset et al., 1992; Radtmacher et al., 1998; Rocca et al., 2002). The MTR is the quantitative measure of the amount of MT that occurs between the bound and the mobile water molecules in a given ROI.

Studies have shown decreased MTR in white matter regions of patients with TBI (Bigler et al., 2010; McGowan et al., 2008) even when there was no observable pathology on conventional imaging (Duckworth and Stevens, 2010; Kimura et al., 1994; Mannen et al., 2009; Sinson et al., 2010). Furthermore, MTI has proven sensitive in detecting changes in patients with even mild brain injury (McGowan et al., 2009). It has been postulated that decreased MTR in TBI may reflect

an increase in concentration of microglia, amyloid, phagocytic vacuoles, and/or other injury products, such as extracellular matrix components within both the gray and white matter. Decreased MTR has been correlated with worse overall outcome in TBI (Sinson et al., 2010) and also with specific neuropsychological deficits (McGowan et al., 2008).

Challenges for MTI include the fact that MTR reflects complex biological conditions that make it difficult to attribute change to a specific pathological process (e.g., edema, Wallerian degeneration or myelin loss). Second, the comparability of results obtained with different scanners or acquisition protocols is undetermined and may be somewhat difficult to establish in multi-site studies (Fagan et al., 2008). Third, MTI sequences can be lengthy and motion artifact can influence data consideration. Finally, as with many advanced techniques, appropriate normative data are required because age-related differences can be substantial, particularly at the extremes of age. Given the sensitivity of DTI data to changes in just about any parameter, such normative data are ideally acquired on the same scanner using the same protocol.

Currently there are numerous commercially and freely available software packages for the processing and analysis of DTI data, and several different analysis methods exist, including (but not limited to) single- or multiple-slice ROI approaches, quantitative tractography, tract-based spatial statistics, voxel-based analysis, and histogram analyses. Each of these forms of analysis has advantages and disadvantages depending upon the question being addressed. A detailed listing of the limitations of each analytic technique is beyond the scope of this review, but researchers should be advised that differences in post-processing and analytic methods may produce differences in the results obtained.

Perfusion imaging

CT perfusion. CT perfusion can be performed by tracking the passage of contrast-labeled blood through the brain following injection of a bolus of water-soluble iodinated contrast medium. Data are typically acquired every 2–3 sec and a time-density curve is constructed. There is a linear relationship between iodine concentration and Hounsfield number, produced over the range of radiation dosages that are typically used to acquire a CT scan of the brain. Quantitative analyses can therefore be performed to estimate the amount of blood flow through the brain as well as other parameters, such as time of first arrival, time to half-max, time to peak, and transit time of the first bolus of contrast-laden blood. These allow for some semi-quantitative estimates of CBF on a voxel-by-voxel basis. However, there is a radiation penalty to be paid for this frequent scanning as well as a (albeit low) morbidity/mortality rate associated with the administration of iodinated contrast media. A few recent studies have examined regional cerebral hemodynamics using perfusion CT in relation to clinical variables such as posttraumatic amnesia in patients with mild brain injury (Metting et al., 2010), and assessment, monitoring, and prognostication in patients with more severe injury (Soustiel et al., 2008; Wintermark et al., 2004a,b).

MRI perfusion. Historically, MR perfusion imaging has been performed using a first pass T2* "dye dilution" technique using a bolus of gadolinium (Gd) contrast and plotting change in signal induced by the contrast-laden blood against time. Integration of the area under the curve gives a measure of the volume of blood passing through an ROI. Other parameters that can be measured include time of arrival, time to peak, and transit time. Alternatively, T1 techniques with a small preparatory dose of Gd prior to the bolus of contrast, to remove T2* effects, can be used in conjunction with compartmental analysis to better understand breakdown of the blood–brain barrier (Wintermark et al., 2005). Because of the need for a contrast agent, MR perfusion is less commonly used in research.

ASL. ASL perfusion MRI is a newer technique for measuring cerebral perfusion that uses arterial blood water as an endogenous contrast agent, negating the need for Gd. In ASL, the protons in arterial blood water are electromagnetically labeled proximal to the tissue of interest and the effects of perfusing are determined by pair-wise comparison with images acquired using control labeling. The rate of decay of the signal from a known band proximal to the tissue of interest can be used qualitatively to compare perfusion of different areas of the brain on the same slice as well as calculate CBF using known parameters of protons in the blood, based on numerical values abstracted from the literature. Study results that are now at least four different variations on ASL including continuous ASL (CASL) (Detre and Alsop, 1999), pulsed ASL (PASL), cPASL (continuous PASL), and velocity selected ASL (VSASL) (Wang et al., 2005).

ASL has been used to study rodent models of TBI (Fisher et al., 1977a,b; Hendrich et al., 1999; Kochanek et al., 2002, 2005; Robertson et al., 2008), and has recently also been used in patient studies (Liu et al., 2010). Several promising potential applications for ASL in the study of TBI have been proposed, including characterization of regional brain function in severe TBI in which task-evoked responses are difficult to obtain; determination of the relationship between changes in regional CBF and cognitive deficits to identify potential targets for pharmacological therapy or other intervention; and use as a biomarker for pharmaceutical therapy (Kochanek et al., 2009). ASL should be especially robust in children as the smaller head size, higher intrinsic brain water, faster inherent blood flow rate, and typical absence of stenoses or atherosclerosis all lead to an increase in intensity of tracer signal. Perfusion parameters that can be developed from ASL include quantitative CBF as well as transit times and the possibility of measuring extraction fractions. ASL has also been used to perform fMRI. ASL may be of interest both in acute mild TBI as well as during the sub-acute and later phases of recovery from more moderate-to-severe TBI.

Other advanced forms of MRI

fMRI, including resting state. The sensitivity of fMRI is based on the blood oxygen level dependent (BOLD) technique resulting in the observation that when neurons are activated, there is an oversupply of arterial blood diverted to that region. The results in an overabundance of oxygenated blood in the venous effluent coming away from that area of the brain. The resulting alteration in oxy- to deoxy-hemoglobin changes the paramagnetic/diamagnetic properties of the tissue, which can be exercised using a T2* acquisition. Using an appropriate paradigm (e.g., an 8 Hz flashing and rotating checkerboard in the case of stimulation of the visual cortex), the stimulus may be applied using a box car (or event-related) design with

appropriate alternating periods of rest and stimulation, which can later be subtracted to remove background noise. The acquired results of a series of repeated stimuli are summed and subtracted to increase the robustness of the data and statistical parametric maps derived (using a program such as statistical parametric mapping [SPM] or analysis of functional neuroimages [AFNI]) which can then be re-applied to a high spatial resolution matching T1-weighted anatomic slice fMRI has been used to examine functional activation patterns in patients with TBI at all levels of severity in both adults (Caljuka et al., 2006; Christodoulou et al., 2001; Marquis et al., 2007; McAllister et al., 1999, 2001; Newsome et al., 2007c; Perlstein et al., 2004; Rasmussen et al., 2009; Scheibel et al., 2003, 2007; Schmitz et al., 2006; Soeda et al., 2005) and children (Levelli et al., 2007; Newsome et al., 2007b; Scheibel et al., 2003). fMRI may also be important in understanding recovery from mild TBI (Chen et al., 2004, 2007, 2008; Jantzen et al., 2004; Lovell et al., 2005) or in rehabilitation efforts in more severe forms of TBI (Kim, Y. H. et al., 2009; Lasbleb, L. et al., 2004a,b; Strangman et al., 2005, 2008).

More recently, there has been increasing interest in the concept of brain "default" areas active at rest, and data have been collected with a subject in the scanner using the BOLD technique but without any stimulus. This resting fMRI (rfMRI) data have been analyzed to look for neural networks or areas of connectivity (reMRI) within the brain. There are currently two published ways in which this has been performed: 1) by identifying clusters of voxels with high "activation" using a priori knowledge of 8 predesignated nodes (James et al., 2009); and 2) by applying independent component analysis (ICA) (Calhoun et al., 2002) to look for connectivity within different areas of the brain. Functional connectivity has been recently applied in both mild TBI (Meyer et al., 2011) and more severe TBI (Marquez de la Plata et al., 2011) and understanding the coherence of functional networks may provide important insights into recovery and therapeutic issues as a biomarker for pharmaceutical therapy (Kochanek et al., 2009). ASL should be especially robust in children as the smaller head size, higher intrinsic brain water, faster inherent blood flow rate, and typical absence of stenoses or atherosclerosis all lead to an increase in intensity of tracer signal. Perfusion parameters that can be developed from ASL include quantitative CBF as well as transit times and the possibility of measuring extraction fractions. ASL has also been used to perform fMRI. ASL may be of interest both in acute mild TBI as well as during the sub-acute and later phases of recovery from more moderate-to-severe TBI.

Other advanced forms of MRI

fMRI, including resting state. The sensitivity of fMRI is based on the blood oxygen level dependent (BOLD) technique resulting in the observation that when neurons are activated, there is an overabundance of arterial blood diverted to that region. The results in an overabundance of oxygenated blood in the venous effluent coming away from that area of the brain. The resulting alteration in oxy- to deoxy-hemoglobin changes the paramagnetic/diamagnetic properties of the tissue, which can be exercised using a T2* acquisition. Using an appropriate paradigm (e.g., an 8 Hz flashing and rotating checkerboard in the case of stimulation of the visual cortex), the stimulus may be applied using a box car (or event-related) design with

Studies using proton MRS in children have found similar neurometabolite alterations after injury. Typically, N-acetyl aspartate (NAA), an amino acid synthesized in mitochondria, is a neuronal and axonal marker that is reduced as a result of neuronal loss or dysfunction after injury. Several studies have shown a direct correlation of reduced NAA and impaired long-term neuropsychological function in children (Babikian et al., 2005; Brenner et al., 2003; Hunter et al., 2005; Yeo et al., 2006). Total choline (Cho) primarily consisting of phosphocyl and glycerophosphocyl Cho is elevated because of shearing of myelin and cellular membranes (diffuse axonal injury) and/or repair. Total creatine (Cr) composed of Cr and phosphocreatine, is assumed to be fairly constant, however recent studies have shown that Cr changes in various disease states (Hattingen et al., 2008; Ingrisch et al., 2003; Munoz Maniega et al., 2008) including TBI (Gasparovic et al., 2009). Lactate (Lac) accumulates as a result of anaerobic glycolysis and in the setting of TBI may be a response to release of glutamate (Alessandri et al., 2003). Studies have shown that lactate presence is more common in children after non-accidental TBI than after accidental TBI (Aaen et al., 2010; Ralphsmeyer et al., 1997) and is strongly correlated with poor outcome in both groups. Glutamate and immediately formed glutamine (Gln) are excitatory amino acid neurotransmitters released to the extracellular space after brain injury that play a major role in neuronal death (Ashwal et al., 2004a; Bullock et al., 1998). Myoinositol (Ins), an organic osmolyte located in astrocytes, increases as a result of glial proliferation and has been correlated with poor outcome after TBI (Ashwal et al., 2004a; Gerrath et al., 2001). Lipids and macromolecules (Lip+MM) produce broad peaks in a spectrum and may increase as a result of severe brain injury, because of a breakdown of cell membrane and release of fatty acids (Panigrahy et al., 2010).

MRS has benefited in the last few years from advances in technology and software development. Scanner manufacturers provide spectroscopy packages with standard sequences such as point resolved spectroscopy (PRESS) and stimulated echo acquisition mode (STEAM) to be used with techniques such as single voxel spectroscopy (SVS), which allows acquisition of a single spectrum from one volume element (voxel), and 2- or 3-D magnetic resonance spectroscopic imaging (2D-MRSI/3D-MRSI), also called chemical shift imaging (CSI), which allows simultaneous acquisition of multiple spectra in a defined ROI through multiple slabs in the brain. MRSI provides more information than SVS but also requires more acquisition time, which must always be considered when imaging children. However, higher field strengths with better signal-to-noise, multi-channel head coils, and advanced sequences are being used to shorten acquisition times. Manufacturers have also incorporated automatic water suppression and shimming, outer volume fat saturation bands, and post-processing software into their spectroscopy packages to facilitate clinical use of MRS.

The field strength, the type of sequence and the parameters used such as the TR (repetition time) and the echo delay time (TE) determine the appearance of the spectrum and the metabolites that can be detected. In order to compare findings from one institution to another, strict protocols must be used not only for spectral acquisition, but also for the post-processing, which greatly affects the information displayed in the spectrum. Spectral processing identifies metabolites according to their chemical shift resonance and measures the area under each

peak, proportional to their concentration. The findings are often reported as peak area metabolite ratios such as NAA/Cr or Cho/Cr. The distribution of metabolite levels or ratios acquired with MRSI displayed as signal intensities for each voxel and overlayed onto anatomic images, are known as metabolite maps or images. Previously, it was thought that Cr (the creatine phosphocreatine (Cr/PCr) pool) is constituent of a constant level in the brain, and is therefore used in many studies as an internal reference standard. Although it is known that Cr levels can change in certain conditions, ratios continue to be useful for reporting and comparing serial measurements or data among institutions using similar acquisition and analysis techniques, and has advantage that correction for partial volume signal intensity loss and signal intensity calibrations are not required (Govind et al., 2010). Quantitation of MR spectra to determine absolute metabolite concentrations, however, is being used more commonly. Quantitative methods use water as an internal reference (Barker et al., 1993) or phantoms containing known metabolite concentrations to quantify peak areas and report absolute or relative metabolite concentrations rather than ratios (Kreis et al., 2010; Danielsen and Henriksen, 1994; Provencher, 1993). It is also becoming more common to use segmentation (McLean et al., 2000) and linear regression (Schuff et al., 2001) techniques to estimate the contributions to metabolite signal arising from both gray and white matter within the same voxel, as well as CSF that minimize signal loss.

P^{31} phosphorus MRS has been used historically to look at energy metabolites, but suffers from long acquisition times. Phosphorus MRS can also be used to calculate pH of tissue. In the future, fixed parity wavelet, tunnable band-pass will expand the multi-nuclear capability of MRS in conventional scanners and also allow for emerging techniques such as hyperpolarization imaging (described subsequently).

Other considerations for study design to be aware of before using MRS, are that metabolite levels vary by anatomic region (Frahm et al., 1989) and change rapidly as the brain develops (Kreis et al., 1993) requiring the use of normal age-matched reference data for interpreting MR spectra from children. At birth, NAA and Cr levels are low, whereas Cho and Ins are high. NAA and Cr increase rapidly with normal brain maturation in the first 18–24 months of life at the same time that Cho and Ins are decreasing rapidly, with all metabolites leveling off at near adult levels by 24 months (Kreis et al., 1993; Ross et al., 1998). However, NAA continues to rise slightly, peaking at ~ 13–15 years, and then decreases slightly over time as the number of neurons and axons gradually declines with normal aging, whereas Cr continues to slightly increase after reaching adult levels (Kreis et al., 1993). Although normal age-related metabolite levels and ratios have been published (Holshouser et al., 1997; Huppi et al., 1991; Pouwels et al., 1998), most institutions establish their own control values for comparison to patient studies, as values may vary with specific scanners, field strengths, and protocols.

MRS holds great promise for TBI evaluation as it provides a sensitive, noninvasive assessment of neurochemical alterations after brain injury, and has shown metabolic abnormalities in regions of the brain that appear normal on conventional MRI sequences (Garnett et al., 2000; Holshouser et al., 2005). However, similar to DTI, the post-processing and analysis of MRS is more complicated, and the expertise needed to establish an MRS program may not be available at all institutions. The challenge is to establish standard, automated techniques and protocols so that MRS can be routinely incorporated into the evaluation of patients with TBI. To this end, manufacturers are already providing proton MRS software packages that require minimal training to use with standard sequences and fully automated shimming, water suppression, and reference scaling. In addition, commercially available packages for automated spectral fitting and processing are already available and widely used. An initial approach for multi-center studies may be to use single-voxel MRS with a standard sequence (such as PRESS with short echo time) that minimizes high signal-to-noise and enables acquisition of short T2 relaxation time metabolites with relatively short acquisition times. These sequences can be acquired in minutes followed immediately by a water reference spectrum requiring only seconds, to enable metabolite quantification. Spectral fitting and automated output of metabolite results can then be done with a commercially available fully automated, user-independent spectral fitting package. LCModel is one of the most widely used packages and includes automated baseline and phase correction, and allows absolute quantification with appropriate calibration as well as an estimate of the uncertainty of the fit (Provencher, 1993). The automated output of metabolite concentrations (i.e., NAA, Cr, Cho, Ins, Glu), the fit estimate that would be used as an indication of the quality of the spectra, and the pertinent acquisition information (i.e., TR, TE, voxel size, brain region) within the same voxel, as well as CSF that minimize signal loss.

P^{31} phosphorus MRS has been used historically to look at energy metabolites, but suffers from long acquisition times. Phosphorus MRS can also be used to calculate pH of tissue. In the future, fixed parity wavelet, tunnable band-pass will expand the multi-nuclear capability of MRS in conventional scanners and also allow for emerging techniques such as hyperpolarization imaging (described subsequently).

Other considerations for study design to be aware of before using MRS, are that metabolite levels vary by anatomic region (Frahm et al., 1989) and change rapidly as the brain develops (Kreis et al., 1993) requiring the use of normal age-matched reference data for interpreting MR spectra from children. At birth, NAA and Cr levels are low, whereas Cho and Ins are high. NAA and Cr increase rapidly with normal brain maturation in the first 18–24 months of life at the same time that Cho and Ins are decreasing rapidly, with all metabolites leveling off at near adult levels by 24 months (Kreis et al., 1993; Ross et al., 1998). However, NAA continues to rise slightly, peaking at ~ 13–15 years, and then decreases slightly over time as the number of neurons and axons gradually declines with normal aging, whereas Cr continues to slightly increase after reaching adult levels (Kreis et al., 1993). Although normal age-related metabolite levels and ratios have been published (Holshouser et al., 1997; Huppi et al., 1991; Pouwels et al., 1998), most institutions establish their own control values for comparison to patient studies, as values may vary with specific scanners, field strengths, and protocols.

MRS holds great promise for TBI evaluation as it provides a sensitive, noninvasive assessment of neurochemical alterations after brain injury, and has shown metabolic abnormalities in regions of the brain that appear normal on conventional MRI sequences (Garnett et al., 2000; Holshouser et al., 2005). However, similar to DTI, the post-processing and analysis of MRS is more complicated, and the expertise needed to establish an MRS program may not be available at all institutions. The challenge is to establish standard, automated techniques and

SPECT. Consequently, distribution patterns may be mapped by injection and imaging of several hyperpolarized C^{13} metabolites simultaneously giving valuable information about membrane structure and permeability. These has already been proof of concept in the pulmonary system in adults using Xe^{129} (Kaushik et al., 2010) and translation into the pediatric population is anticipated, allowing us to enter the world of molecular imaging, proteomics, and genomics.

Nuclear medicine

SPECT. SPECT imaging is performed by collecting data from a gamma-emitting isotope (e.g., Tc^{99}m), by use of a gamma camera to acquire multiple 2D images. This process typically takes ~ 20 min in order to obtain enough signal-to-noise. Using a computer and applying a tomographic reconstruction algorithm to the multiple projections, a 3D data set is produced that can then be manipulated and reconstructed in any plane, producing images in a similar fashion to those produced by other tomographic techniques such as CT, MRI, and PET.

Following injection, Tc^{99}m-labelled tracers such as hexamethylpropylene amine oxime (HMPAO) are taken up by brain tissue in a manner proportional to CBF and can therefore be used to assess brain tissue flow. Because blood flow to the brain is tightly coupled to local brain energy use, this information can be used as an indirect measure of regional brain metabolism. Recent studies have shown the accuracy of SPECT in Alzheimer's disease to be as high as 88% (Binetti et al., 2000). Tc^{99}m is a metastable nuclear isomer that is readily available in most hospitals, and easy and cheap to produce. SPECT has been used in TBI to examine recovery (Chiu Wong et al., 2006).

PET. Whereas SPECT uses radioactive tracer materials that emit gamma radiation directly, PET tracers (eg., F^{18} deoxyglucose (FDG)) emit positrons that annihilate with electrons up to a few millimeters away, causing two gamma photons to be emitted at 180 degrees to each other. The PET scanner detects these emissions "coincident" in time, providing more localization information and therefore higher spatial resolution images than SPECT (~1 cm resolution).

FDG PET scanning of the brain measures regional brain glucose metabolism and can provide information concerning focal brain damage. The information extracted is not dissimilar to that obtained from Tc^{99}m HMPAO SPECT imaging which is, however, more freely and cheaply available. Limited studies have been used PET in TBI (Bernstein et al., 2009; Hattori et al., 2003, 2004; Kato et al., 2007). O^{15} has also been used to measure CBF and oxygen extraction fraction. As with all techniques involving radiation, consideration has to be given to the dose received by the patient, and therefore limits the performance of serial examinations.

Mini-cyclotrons have been developed over the last 10 years that enable positron emitters to be produced locally, thereby removing dependence on a few major centers with a cyclotron. However the cost of the radiopharmaceuticals that resemble a feel-lab, on-site chemist and selection of a special site (e.g., basement or ground floor) for extraction of any cadaverous gases is question. MRI is capable of identifying signal from the tracer made (e.g., C^{13}) in different molecules, unlike PET/

and combine both pieces of equipment to further improve localization of isotope activity by better enabling registration of images from both modalities. More recently, early work with PET/MRI scanners has been performed, but there remain numerous obstacles to overcome before these will be available for routine clinical use.

Other techniques

Electroencephalography (EEG). EEG and amplitude EEG (aEEG) are the current techniques used in clinical practice to monitor effects on the electrical activity of the brain following TBI, and for the earliest detection of seizure activity. For the purposes of epilepsy surgery that may occur in the post-traumatic setting, EEG has been co-registered with fMRI for the purposes of improved localization of foci of seizure activity. EEG has also been used to examine TBI-related disruption of the blood–brain barrier (Korn et al., 2005; Tomkins et al., 2011).

MEG/MMS. MEG is a method of recording magnetic flux on the surface of the head that is associated with intracranial electrical currents produced between synapses or within the axons or dendrites of neurons. Similar to EEG and evoked potentials (EPs) recordings, it can be used to detect abnormalities in spontaneous brain activity. However, MEG can also be used for localization and estimation of the cortex and time course for these kinds of signals, and allow construction of images of brain activity, a process that is often referred to as MSI. Because of its high degree of resolution of normal and abnormal brain physiology for both spatial and temporal resolution, MSI has been considered a potentially useful tool in TBI-related research (Bigler, 1999), particularly for diagnosis of milder TBI for which MR findings are unrevealing (Huang et al., 2009; Lewine et al., 1999, 2007).

However, significant challenges remain in the use of MEG/MSI. Most importantly, few medical centers have access to magnetometers or gradiometers, and analysis of the data requires specialized expertise. Usually limiting its widespread use as either a clinical or a research tool. Second, although the temporal resolution of MEG is excellent, variations in signaling can be introduced through a number of sources (eg., external stimulation, movement, unrelated mental activity); therefore, challenges exist related to its use in acute or severe TBI, because drowsiness, suboptimal levels of cooperation, and states of altered consciousness may limit the robustness of findings. MSI is best used for measurement of surface cortical activity; depending upon the modeling used, regions such as the basal temporal regions or the sub-cortical regions may be substantially more difficult to accurately measure.

Future Issues and Research Needs

The Pediatric CDE Workgroup identified several challenges and areas in which additional research would enhance the use of advanced imaging techniques in TBI. First, the pace of technological advance has provided both tools that allow significant advances in the understanding of TBI, and also with time- and resource-efficient analysis tools for large data sets. However, it is primarily the rapidity at which advanced forms of neuroimaging evolves that has also decreased the distinction that a single, common protocol or set of analysis tools would remain in use for many years at a time.

Even evaluation of the emerging elements may need to reflect the pace at which things change to optimize certain kinds of discovery, but may also limit the amount of data that can be collected under any given version of the recommendations made by the Workgroup. Additional work is needed to consider adjustments that can be made to better "square" measurements derived from older data. At this time, specific protocols for most of the advanced imaging techniques have not been established, and this remains an area of future need.

At present, significant challenges remain in ensuring comparability between data acquired on magnets of different manufacturers or using different versions of instrumentation, equipment, or software. Creation of large normative data sets would be a tremendous contribution to understanding TBI-related changes, particularly in the context of development, but this remains a challenging issue for some of the advanced modalities, given the issues previously mentioned. The acquisition of advanced imaging data can also be a significant expense, and data storage requirements should be considered, which also limits the amount of data that are currently collected for clinical trials and large multi-site studies in patients. However, technology has also aided in providing more cost-effective solutions to data acquisition, storage, and processing, and the evolution of these may result in further reduction in cost and the availability of fewer resources to a greater number of investigators.

Conclusions

The diversity of imaging for use in TBI is evidenced by this article. Although MRI is currently the mainstay of instrumentation for both current and emerging techniques, other methodologies are also available CT and nuclear medicine techniques have the drawback of an accompanying radiation dose, but at present offer some complimentary information regarding the detection of acute subarachnoid hemorrhage and bone injury, and real-time metabolism, respectively. Electrophysiological techniques such as MEG and MSI (when combined with MRI) are already revealing new information concerning acute mild TBI, which is the most ubiquitous of all brain injuries. New and emerging hyperpolarization experiments performed on current MR scanners have a fascinating potential insight into the world of molecular imaging that has yet to be fully realized with respect to the brain. Multimodal imaging enables more comprehensive, more extensive, as different forms of imaging may provide unique insights into the nature of injury to the brain and the course of recovery. More advanced methods of integrating different imaging modalities, together with genetic information and the results of neurocognitive testing, should provide a very powerful set of tools for better understanding the pathophysiology underlying TBI, allowing for more accurate prognostication and the possibility of individualizing for new and future interventions with ultimate improvement in patient outcomes. Currently, the Workgroup is developing a "toolbox" that allows for the establishment of potentially reproducible quantitative measures that can be used to determine the extent of injury as well as assess new interventions and therapies for the sequelae of TBI as they arise. Additionally, efforts are underway to evaluate the utility of different commercially available software and public domain tools that may be very helpful in processing data, as these may provide an excellent basis for

ging I. (2010). Ventricular maps in 804 ADNI subjects: correlations with CSF biomarkers and clinical decline. Neurobiol. Aging 31, 1386–1400.

Christodoulou, C., DeLuca, J., Ricker, J.H., Madigan, N.K., Bly, B.M., Lange, G., Kalnin, A.J., Liu, W.C., Steffener, J., Diamond, B.J., and Ni, A.C. (2001). Functional magnetic resonance imaging of working memory impairment after traumatic brain injury. J. Neurol. Neurosurg. Psychiatry 71, 161–168.

Colon, L.P. (2007). Imaging after brain injury. Br. J. Anaesth. 99, 49–60.

Danielsen, E.R., and Henriksen, O. (1994). Absolute quantitative proton NMR spectroscopy based on the amplitude of the first water suppression pulse. Quantification of brain water and metabolites. NMR Biomed. 7, 313–319.

Detre, J.A., and Alsop, D.C. (1999). Perfusion magnetic resonance imaging with continuous arterial spin labeling: methods and clinical applications in the central nervous system. Eur. J. Radiol. 30, 115–124.

Ding, K., Marquez de la Plata, C., Wang, J.Y., Mumphrey, M., Moore, C., Harper, C., Madden, C.J., McColl, R., Whetsell, W., Devous, M.D., and Diaz-Arrastia, R. (2008). Cerebral atrophy after traumatic white matter injury: correlation with acute neuroimaging and outcome. J. Neuropathol. Exp. Neurol. 67, 1130–1139.

Dinomais, V., Reynaud, C., Rahmani, R.I., Renou, P.Y., Schvartz, M., Saliba, E., Gouyet, L.H., Gonzalez-Scarano, F., Lavi, E., and Cohen, J.A. (1992). Experimental allergic encephalomyelitis and multiple sclerosis: lesion characterization with magnetization transfer imaging. Radiology 182, 483–491.

Duckworth, J.L., and Stevens, R.D. (2010). Imaging brain trauma. Curr. Opin. Crit. Care 16, 93–97.

Dumais, D., Huynh, L., Filiard, F., Remisz, J., Petit-Lacour, M.C., Manoch-Dupuch, K., and Lagueniere, F. (2005). Brain MR diffusion tensor imaging and fiber tracking to differentiate between non diffuse axonal injuries. Neuroradiology 47, 604–608.

Dufresne, A.C., Gean, A.D., Hoarke, L.M., Hicks, R., Wintermark, M., Mukherjee, P., Lee, S., Tong, K.A., Buck, C.R., and Common Data Elements Neuroimaging Working Group Members FWGM (2010). Common data elements in radiologic imaging of traumatic brain injury. Arch. Phys. Med. Rehabil. 91, 1661–1666.

Dufresne, A.C., Holshouser, B., Hunter, J.V., Tong, K.A. (2011). Common data elements for neuroimaging of traumatic brain injury: preliminary considerations in pediatric moderate and severe traumatic brain injury. Brain Inj. 25, 1019–1028.

Ewing-Cobbs, L., Prasad, M.R., Swank, P., Kramer, L., Cox, C.S., Jr., Fletcher, J.M., Baumgartner, J., Zhang, X., and Hasan, K.M. (2008). Acute callosal development and 12-month cognitive outcome following pediatric traumatic brain injury: relation to neurobehavioral indicators. Neuroimage 42, 1305–1315.

Fearing, M.A., Bigler, E.D., Gale, S.D., Johnson, S.C., Hunter, J.V., Xiaoqi, L., Hunter, G., and Levin, H.S. (2008). Morphometric MRI findings in the thalamus and brainstem in children after moderate to severe traumatic brain injury. J. Child Neurol. 23, 729–737.

Fenton, M.L., Hendrich, K.S., Kocsmaski, P.M., Williams, D.S., Schilling, J.K., Wisniewski, S.R., Kelsey, S.F., DeKosky, S.T., Graham, S.H., Marion, D.W., and Ho, C. (1999). Assessment of cerebral blood flow and CO2 reactivity after controlled cortical impact by perfusion magnetic resonance imaging using arterial spin labeling in rats. J. Cereb. Blood Flow Metab. 17, 805–814.

Fenton, M.L., Hendrich, K.S., Schilling, J.K., Williams, D.S., Ho, C., DeKosky, S.T., Marion, D.W., and Kochanek, P.M. (1998). Perfusion MRI assessment of cerebral blood flow and CO2 reactivity after controlled cortical impact in rats. Adv. Exp. Med. Biol. 411, 7–12.

Frahm, J., Bruhn, H., Gyngell, M.L., Merboldt, K.D., Hanicke, W., and Sauter, R. (1989). Localized proton NMR spectroscopy in different regions of the human brain in vivo. Relaxation times and concentrations of cerebral metabolites. Magn. Reson. Med. 11, 47–63.

Friedman, L., and Glover, G.H. (2006). Report on a multicenter fMRI quality assurance protocol. J. Magn. Reson. Imaging 23, 827–839.

Friedman, L., Stern, H., Brown, G.G., Mathalon, D.H., Turner, J., Glover, G.H., Gollub, R.L., Lauriello, J., Lim, K.O., Cannon, T., Greve, D.N., Bockholt, H.J., Belger, A., Mueller, B., Doty, M.J., He, J., Wells, W., Smyth, P., Pieper, S., Kim, S., Kubicki, M., Vangel, M., and Potkin, S.G. (2008). Test-retest and between-site reliability in a multicenter fMRI study. Hum. Brain Mapp. 29, 958–972.

Garnett, M.R., Blamire, A.M., Corkill, R.G., Cadoux-Hudson, T.A., Rajagopalan, B., and Styles, P. (2000). Early proton magnetic resonance spectroscopy in normal-appearing brain correlates with outcome in patients following traumatic brain injury. Brain 123, 2046–2054.

Garnett, M.R., Corkill, R.G., Blamire, A.M., Rajagopalan, B., Manners, D.N., Young, J.D., Styles, P., and Cadoux-Hudson, T.A. (2001). Altered cellular metabolism following traumatic brain injury: a magnetic resonance spectroscopy study. J. Neurotrauma 18, 231–240.

Gasparovic, C., Yeo, R., Mannell, M., Ling, J., Elgie, R., Phillips, J., Doezema, D., and Mayer, A.R. (2009). Neurometabolite concentrations in gray and white matter in mild traumatic brain injury: an 1H-magnetic resonance spectroscopy study. J. Neurotrauma 26, 1635–1643.

Gerber, D.J., Weinraub, A.M., Cusick, C.P., Sicri, P.K., and Whitsenck, G.G. (2004). Magnetic resonance imaging of mesiotemporal injury: relationship of T2/SE and TSE to clinical severity and outcome. Brain Inj. 18, 1083–1097.

Govind, V., Gold, S., Kaliannan, K., Saigal, G., Falcone, S., Arheart, K.L., Harris, L., Jagid, J., and Maudsley, A.A. (2010). Whole-brain proton MR spectroscopic imaging of mild-to-moderate traumatic brain injury and correlation with neuropsychological deficits. J. Neurotrauma 27, 483–496.

Green, R.E., Turkstra, L.S., van der Casig, R.J., and Ziviani, M.F. (2010). Pervasive sociocortical abnormalities in autism: a DTI study. J. Psychiatry Neurosci. 36, 32–40.

Haacke, E.M., Duhaime, A.C., Gean, A.D., Riedy, G., Wintermark, M., Mukherjee, P., Brody, D.L., DeCrespigny, T., Duncan, T.D., Hertle, R., Hertle, L., Latour, L., Stolmaskopoulos, J.C., and Smith, D.H. (2010). Common data elements in radiologic imaging of traumatic brain injury. J. Magn. Reson. Imaging 32, 516–543.

Haacke, E.M., Xu, Y., Cheng, Y.C., and Reichenbach, J.R. (2004). Susceptibility weighted imaging (SWI). Magn. Reson. Med. 52, 612–618.

Hattiangadi, E., Rasb, P., Fuetz, K., Lemiemann, H., Seize, M., Gerlach, R., Zanella, F.E., and Plastas, U. (2008). Prognostic value of choline and creatine in WHO grade II gliomas. Neuroradiology 50, 759–767.

Hattori, N., Huang, S.C., Wu, H.M., Liao, W., Glenn, T.C., Vespa, P.M., Phelps, M.E., Hovda, D.A., and Bergsneider, M. (2004). Acute changes in regional cerebral [18F-FDG] kinetics in patients with traumatic brain injury. J. Nucl. Med. 45, 775–783.

Hattori, N., Huang, S.C., Wu, H.M., Yeh, E., Glenn, T.C., Vespa, P.M., McArthur, D., Phelps, M.E., Hovda, D.A., and Bergsneider, M. (2003). Correlation of regional metabolic rates of glucose with glasgow coma scale after traumatic brain injury. J. Nucl. Med. 44, 1709–1718.

Hendrich, K.S., Kochanek, P.M., Williams, D.S., Schiding, J.K., Marion, D.W., and Ho, C. (1995). Early perfusion after controlled cortical impact in rats: quantification by arterial spin-labeled MRI and the influence of apparent transit time heterogeneity. Magn. Reson. Med. 42, 673–681.

Hillary, F.G., Steffener, J., Newell, R.S., Lange, G., DeLuca, J., and Ashburner, J. (2002). Functional magnetic resonance imaging technology and traumatic brain injury rehabilitation: guidelines for methodological and conceptual pitfalls. J. Head Trauma Rehabil. 23, 15–22.

Hinzman, L., Puttin, R., Ioannou, N., Hefernan, H., Kurki, T., and Tenovuo, O. (2003). Cognitive functions in relation to MRI findings 30–70 years after moderate brain trauma. Brain Inj. 17, 93–108.

Holshouser, B.A., Ashwal, S., Luh, G.Y., Shu, S., Kahlon, S., Auld, K.L., Tomasi, S.O., Perkin, R.M., and Hinshaw, D.B., Jr. (1997). Proton MR spectroscopy after acute central nervous system injury: outcome prediction in neonates, infants, and children. Radiology 202, 487–496.

Holshouser, B.A., Tong, K.A., and Ashwal, S. (2005). Proton MR spectroscopy after acute central nervous system injury: outcome prediction in children with traumatic brain injury. AJNR Am. J. Neuroradiol. 26, 1279–1293.

Hsu, Y., Lebar, D.F., Lee, S., Tipp, A.W., Jick, C.R., Jr., Widmer, M.W., Thompson, P.M., and Alzheimer's Disease Neuroimaging I. (2010). Sex and age differences in atrophic rates: an ADNI study with n=1368 MRI scans. Neurobiol. Aging 31, 1463–1480.

Huang, M.X., Theilmann, R.J., Robb, A., Angeles, A., Nichols, S., Drake, A., D'Andrea, J., Levy, M., Holland, M., Song, T., Ge, S., Hwang, E., Yoo, K., Cui, L., Baker, D.G., Trauner, D., Coimbra, R., and Lee, R.R. (2009). Integrated imaging approach with MEG and DTI to detect mild traumatic brain injury in military and civilian patients. J. Neurotrauma 26, 1213–1226.

Huisman, T.A., Schwamm, L.H., Schaefer, P.W., Koroshetz, W.J., Shetty-Alva, N., Ozsunar, Y., Wu, O., and Sorensen, A.G. (2004). Diffusion-weighted imaging as potential biomarker of white matter injury in diffuse axonal injury. AJNR Am. J. Neuroradiol. 25, 370–376.

Hunter, J.V., Thornton, R.J., Wang, Z.J., Levin, H.S., Robertson, G., Brown, M.M., and Swank, P.R. (2005). Late pediatric MR spectroscopy in children after traumatic brain injury: correlation with cognitive outcomes. AJNR Am. J. Neuroradiol. 26, 402–408.

Huppi, P.S., Posse, S., Lazeyras, F., Burri, R., Boxe, E., and Herschkowitz, N. (1991). Magnetic resonance in preterm and term newborns: 1H-spectroscopy in developing human brain. Pediatr. Res. 29, 574–579.

Hutchinson, E., Pulsipher, D., Dobbs, R., Myers-y-Cuitierrez, A., Shelly, R., Jones, J., Seidenberg, M., Hayerwell, E., and Hermann, B. (2009). Children with new-onset epilepsy exhibit diffusion abnormalities in cerebral white matter in the absence of volumetric differences. Epilepsy Res. 86, 208–214.

Inglese, M., Li, B.S., Rusinek, H., Babb, J.S., Grossman, R.I., and Gonen, O. (2003). Diffusely elevated cerebral choline and creatine in relapsing-remitting multiple sclerosis. Magn. Reson. Med. 50, 190–195.

Jones, C.A., Kelley, M.K., Craddock, R.C., Holtzheimer, P.E., Dunlop, B.W., Nemeroff, C.B., Mayberg, H.S., and Hu, X.P. (2009). Exploratory structural equation modeling of resting-state fMRI: applicability of group models to individual subjects. Neuroimage 45, 778–787.

Jonsson, B.J., Andersen, P., Stridsberg, P.L., and Kelso, J.A. (2004). A prospective functional MR imaging study of mild traumatic brain injury in elite football players. AJNR Am. J. Neuroradiol. 25, 738–745.

Kato, T., Nakayama, N., Yasokawa, Y., Okamura, A., Shinoda, J., and Iwama, T. (2007). Statistical image analysis of cerebral glucose metabolism in patients with cognitive impairment following diffuse traumatic brain injury. J. Neurotrauma 24, 919–926.

Kaushik, S.S., Cleveland, Z.I., Cofer, G.P., Metz, G., Beaver, D., Nouls, J., Kraft, M., Auffermann, W., Wolber, J., McAdams, H.P., and Driehuys, B. (2010). Diffusion-weighted hyperpolarized (129)Xe MRI in healthy volunteers and subjects with chronic obstructive pulmonary disease. Magn. Reson. Med 65, 1154–1165.

Kim, J., Whyte, J., Patel, S., Avants, B., Europa, E., Wang, J., Slattery, J., Gee, J.C., Coslett, H.B., and Detre, J.A. (2010). Resting cerebral blood flow alterations in chronic traumatic brain injury: an arterial spin labeling perfusion FMRI study. J. Neurotrauma 27, 1399–1411.

Kim, Y.H., Yoo, W.K., Ko, M.H., Park, C.H., Kim, S.T. and Na, D.L. (2009). Plasticity of the attentional network after brain injury and cognitive rehabilitation. Neurology Neural Plasticity 23, 468–477.

Kirwan, H., Mesney, D.F., McGowan, J.C., Grossman, R.I., Lenkinski, R.E., Kim, D.T., McIntosh, T.K., Constantini, T.A., and Smith, D.H. (1996). Magnetization transfer imaging of diffuse axonal injury following experimental brain injury in the pig: characterization by magnetization transfer ratio with histopathologic correlation. J. Comput. Assist. Tomogr. 20, 540–546.

Kochanek, P.M., Hendrich, K.S., Dixon, C.E., Schiding, J.K., Williams, D.S., and Ho, C. (2002). Cerebral blood flow at one year after controlled cortical impact in rats: assessment by magnetic resonance imaging. J. Neurotrauma 19, 1369–1377.

Kochanek, P.M., Hendrich, K.S., Jackson, E.K., Wisniewski, S.R., Marion, J.A., Shaw, P.M., Janesko, K.L., Zacharia, L., and Ho, C. (2005). Characterization of the effects of adenosine receptor agonists on cerebral blood flow in uninjured and traumatically injured rat brain using continuous arterial spin-labeled magnetic resonance imaging. J. Cereb. Blood Flow Metab. 25, 1667–1677.

Korn, A., Golan, H., Melamed, I., Pascual-Marqui, R., and Friedman, A. (2005). Focal cortical dysfunction and blood–brain barrier disruption in patients with Postconcussion syndrome. J. Clin. Neurophysiol. 22, 1–9.

Kou, Z., Wu, Z., Tong, K.A., Holshouser, B., Benson, R.R., Hu, J., and Haacke, E.M. (2010). The role of advanced MR imaging findings in forecasting the outcome of traumatic brain injury. J. Head Trauma Rehabil. 25, 367–382.

Kraus, M.F., Susmaras, T., Caughlin, B.P., Walker, C.J., Sweeney, J.A., and Little, D.M. (2007). White matter integrity and cog-

...ability in chronic traumatic brain injury: a diffusion tensor imaging study. Brain 130, 2508–2519

Kreis, R., Ernst, T., and Ross, B. (1993). Absolute quantitation of water and metabolites in the human brain. II. Metabolite concentrations. J. Magn. Reson. 102, 9–19.

Kumar, R., Gupta, R.K., Rao, S.B., Chawla, S., Husain, M., and Rathore, R.K. (2005). Magnetization transfer and T1 quantification in normal appearing cortical gray matter and white matter adjacent to focal abnormality in patients with traumatic brain injury. Magn. Reson. Imaging 23, 893–899.

Kumar, R., Husain, M., Gupta, R.K., Hasan, K.M., Haris, M., Agarwal, A.K., Pandey, C.M., and Narayana, P.A. (2009). Serial changes in the white matter diffusion tensor imaging metrics in moderate traumatic brain injury and correlation with neuro-cognitive function. J. Neurotrauma 26, 481–495.

Laatsch, L., Little, D., and Thulborn, K. (2004a). Changes in fMRI following cognitive rehabilitation in severe traumatic brain injury: A case study. Rehabil. Psychol. 49, 262–267.

Laatsch, L.R., Thulborn, K.R., Krisky, C.M., Shobat, D.M., and Sweeney, J.A. (2004b). Investigating the neurobiological basis of cognitive rehabilitation therapy with fMRI. Brain Inj. 18, 957–974.

Levin, H.S., Wilde, E.A., Chu, Z., Yallampalli, R., Hanten, G.R., Li, X., Chu, J., Vasquez, A.C., and Hunter, J.V. (2008). Diffusion tensor imaging in relation to cognitive and functional outcome of traumatic brain injury in children. J. Head Trauma Rehabil. 23, 197–208.

Levine, B., Kovacevic, N., Nica, E.I., Cheung, G., Gao, F., Schweizer, M.L., and Black, S.E. (2008). The Toronto traumatic brain injury study: injury severity and quantified MRI. Neurology 70, 771–778.

Lewine, J.D., Davis, J.T., Bigler, E.D., Thoma, R., Hill, D., Funke, M., Sloan, J.H., Hall, S., and Orrison, W.W. (2007). Objective documentation of traumatic brain injury subsequent to mild head trauma: multimodal brain imaging with MEG, SPECT, and MRI. J. Head Trauma Rehabil. 22, 141–155.

Lewine, J.D., Davis, J.T., Sloan, J.H., Kodituwakku, P.W., and Orrison, W.W., Jr. (1999). Neuromagnetic assessment of pathophysiologic brain activity induced by minor head trauma. Am. J. Neuroradiol. 20, 857–866.

Lipton, M.L., Gellella, E., Lo, C., Gold, T., Ardekani, B.A., Shifteh, K., Bello, J.A., and Branch, C.A. (2008). Multifocal white matter ultrastructural abnormalities in mild traumatic brain injury with cognitive disability: a voxel-wise analysis of diffusion tensor imaging. J. Neurotrauma 25, 1335–1342.

Lovell, M.R., Pardini, J.E., Welling, J., Collins, M.W., Bahali, J., Lazar, N., Roush, R., Eddy, W.F., and Boston, J.T. (2007). Functional brain abnormalities are related to clinical recovery and time to return-to-play in athletes. Neurosurgery 61, 352–359; discussion 359–360.

Maikusell, K.L., Cecil, K.M., Care, M., and Ball, W.S., Jr. (2005). Elevated lactate as an early marker of brain injury in inflicted traumatic brain injury. Pediatr. Radiol. 35, 668–676.

Marcotti, A.E., Sisavat, L.A., Maida, A.L., Cassisi, A.A., and Santos, A.C. (2009). Evaluation of delayed neuronal and axonal damage secondary to moderate and severe traumatic brain injury using quantitative MR imaging techniques. AJNR Am. J. Neuroradiol. 30, 947–952.

Marques de la Plata, C.D., Garces, J., Shoko Kaipri, E., Catroux, J., Krahman, E., Pulkkil, E., Spence, J., Devous, M.D., Jr., Moore, C., McColl, R., Madden, C., and Diaz-Arrastia, R. (2011). Deficits in functional connectivity of hippocampal and frontal lobe circuits after traumatic axonal injury. Arch. Neurol. 68, 74–84.

Marquez de la Plata, C.D., Garces, J., Shoko Kaipri, E., Catroux, J., Krahman, E., Pulkkil, E., Spence, J., Devous, M.D., Jr., Moore, C., McColl, R., Madden, C., and Diaz-Arrastia, R. (2011). Deficits in functional connectivity of hippocampal and frontal lobe circuits after traumatic axonal injury. Arch. Neurol. 68, 74–84.

Messalos, M., Mysiaris, M., Nakou, T., and Mavroudis, H. (2007). Compensatory cortical activation during performance of an attention task by patients with diffuse axonal injury: a functional magnetic resonance imaging study. J. Neurol. Neurosurg. Psychiatry 78, 168–173.

Metzdorf, A.A., Dankaerts, A., Alper, J.R., Hall, L.O., Schell, N., Shaffrahn, C., Vu, Y., Ibel, A., Perw, A., Goldgof, D., Gu, Y., Pajaro, R., Rousseau, F., Shwenkreis, K., Saber, B.J., Weber, P., Young, K., and Zhu, X. (2006). Computational processing, display and analysis for in vivo MR spectroscopic imaging. NMR Biomed. 19, 492–502.

Mayer, A.R., Ling, J., Mannell, M.V., Gasparovic, C., Phillips, J.P., Doezema, D., Reichard, R., and Yeo, R.A. (2010). A prospective diffusion tensor imaging study in mild traumatic brain injury. J. Neurol. Neurosurg. Psychiatry 81, 1285–1293.

Mayer, A.R., Mannell, M.V., Ling, J., Gasparovic, C., and Yeo, R.A. (2011). Functional connectivity in mild traumatic brain injury. Hum. Brain Mapp. 32, 1825–1835.

McAllister, T.W., Saykin, A.J., Flashman, L.A., Sparling, M.B., Johnson, S.C., Guerin, S.J., Mamourian, A.C., Weaver, J.B., and Yanofsky, N. (1999). Brain activation during working memory 1 month after mild traumatic brain injury: a functional MRI study. Neurology 53, 1300–1308.

McAllister, T.W., Sparling, M.B., Flashman, L.A., Guerin, S.J., Mamourian, A.C., and Saykin, A.J. (2001). Differential working memory load effects after mild traumatic brain injury. Neuroimage 14, 1004–1012.

McCauley, S.R., Wilde, E.A., Bigler, E.D., Chu, Z., Yallampalli, R., Oni, M.B., Wu, T., Barnes, M.A., Pedroza, C., Vasquez, A.C., Hunter, J.V., and Levin, H.S. (2011). Diffusion tensor imaging of incentive effects in preoperative memory after pediatric traumatic brain injury. J. Neurotrauma 28, 503–516.

McGowan, J.C., Yang, J.H., Pliskin, R.C., Grossman, R.I., Doshi, E.M., Cecil, K.M., and Bagley, L.J. (2003). Magnetization transfer imaging in the detection of injury associated with mild head trauma. AJNR Am. J. Neuroradiol. 21, 875–881.

McLean, M.A., Woermann, F.G., Barker, G.J., and Duncan, J.S. (2000). Quantitative analysis of short echo time (1H-MRS) of cerebral gray and white matter. Magn. Reson. Med. 44, 401–411.

Merkley, T.L., Bigler, E.D., Wilde, E.A., McCauley, S.R., Hunter, J.V., and Levin, H.S. (2008). Diffuse changes in cortical thickness in pediatric moderate-to-severe traumatic brain injury. J. Neurotrauma 25, 1343–1345.

Mortimer, Z., Rodger, J., Lee, S., Bye, B.M., Stewart, R.E., Kesner, B.P., and van der Naalt, J. (2010). Acute cerebral perfusion CT abnormalities associated with posttraumatic amnesia in mild head injury. J. Neurotrauma 27, 2143–2149.

Miles, L., Grossman, R.I., Johnson, G., Babb, J.S., Diller, L., and Inglese, M. (2008). Short-term DTI predictors of cognitive dysfunction in mild traumatic brain injury. Brain Inj. 22, 115–122.

Mueller, S.C., Weiner, M.W., Thal, L.J., Petersen, R.C., Jack, C.R., Jagust, W., Trojanowski, J.Q., Toga, A.W., and Beckett, L. (2005). Ways forward in early detection of Alzheimer's disease: the Alzheimer's Disease Neuroimaging Initiative (ADNI). Alzheimers Dement. 1, 55–66.

Munoz Maniega, S., Cvoro, V., Armitage, P.A., Marshall, I., Bastin, M.E., and Wardlaw, J.M. (2008). Choline and creatine are not reliable denominators for calculating metabolite ratios in acute ischemic stroke. Stroke 39, 2667–2669.

Newcombe, V.F., Williams, G.B., Nortje, J., Bradley, P.G., Harding, S.G., Smielewski, P., Coles, J.P., Maiya, B., Gillard, J.H., Hutchinson, P.J., Pickard, J.D., Carpenter, T.A., and Menon, D.K. (2007). Analysis of acute traumatic axonal injury using diffusion tensor imaging. Br. J. Neurosurg. 21, 360–368.

Newsome, M.R., Scheibel, R.S., Hanten, J.V., Wang, Z.J., Chu, Z., Li, X., and Levin, H.S. (2007a). Brain activation during working memory after traumatic brain injury in children. Neurocase 13, 19–24.

Newsome, M.R., Scheibel, R.S., Steinberg, J.L., Troyanskaya, M., Sharma, R.G., Rauch, R.A., Li, X. and Levin, H.S. (2007b). Working memory brain activation following severe traumatic brain injury. Cortex 43, 59–81.

Ng, S.M., Mukherjee, P., Ghatir, J., Johnson, C., Kobler, R.A., Sarkar, R., Lee, H., Mendez, M., Zimmerman, R.D., Manley, G.T., and McCandless, B.K. (2008). Extent of microstructural white matter injury in postconcussion syndrome correlates with impaired cognitive reaction time: a 3T diffusion tensor imaging study of mild traumatic brain injury. AJNR Am. J. Neuroradiol. 29, 1287–1292.

Niogi, S.N., Mukherjee, P., Ghajar, J., Johnson, C., Kolster, R.A., Sarkar, R., Lee, H., Meeker, M., Zimmerman, R.D., Manley, G.T., and McCandless, B.K. (2008). Extent of microstructural white matter injury in postconcussive syndrome correlates with impaired cognitive reaction time: a 3T diffusion tensor imaging study of mild traumatic brain injury. AJNR Am. J. Neuroradiol. 29, 967–973.

Niogi, S.N., Mukherjee, P., Ghajar, J., Johnson, C., Kolster, R.A., Lee, H., Suh, M., Zimmerman, R.D., Manley, G.T., and McCandless, B.K. (2008). Structural dissociation of attentional control and memory in adults sustaining mild traumatic brain injury. Brain 131, 3209–3221.

Niogi, S.N., Mukherjee, P., Ghajar, J., Johnson, C.E., Kolster, R.A., Sarkar, R., Lee, H., Meeker, M.N., Zimmerman, R.D., Manley, G.T., and McCandless, B.K. (2008). Structural dissociation of attentional control and memory in adults sustaining mild traumatic brain injury. Brain 131, 3209–3221.

Nolin, P., Stipdonk, B., Ouimet, B., Allaire, C., Lavallee, M., Abeare, C.A., Reid, I., and Dupuis, F. (2008). Psychometric validation of the Paced Auditory Serial Addition Test (PASAT) in individuals with moderate to severe traumatic brain injury. Brain Inj. 22, 389–398.

Nolin, P., Stipdonk, B., Ouimet, B., Allaire, C., Lavallee, M., Abeare, C.A., Reid, I., and Dupuis, F. (2008). Psychometric validation of the Paced Auditory Serial Addition Test (PASAT) in individuals with moderate to severe traumatic brain injury. Brain Inj. 22, 389–398.

Nolin, P., Stipdonk, B., Ouimet, B., Allaire, C., Lavallee, M., Abeare, C.A., Reid, I., and Dupuis, F. (2008). Psychometric validation of the Paced Auditory Serial Addition Test (PASAT) in individuals with moderate to severe traumatic brain injury. Brain Inj. 22, 389–398.

Nolin, P., Stipdonk, B., Ouimet, B., Allaire, C., Lavallee, M., Abeare, C.A., Reid, I., and Dupuis, F. (2008). Psychometric validation of the Paced Auditory Serial Addition Test (PASAT) in individuals with moderate to severe traumatic brain injury. Brain Inj. 22, 389–398.

...underlies discordant imaging findings: diffusivity behaves differently in gray and white matter post acute concussion. Acta Neurochirurg. 102, 247–251.

Newcombe, V.F., Williams, G.B., Nortje, J., Bradley, P.G., Harding, S.G., Smielewski, P., Coles, J.P., Maiya, B., Gillard, J.H., Hutchinson, P.J., Pickard, J.D., Carpenter, T.A., and Menon, D.K. (2007). Analysis of acute traumatic axonal injury using diffusion tensor imaging. Br. J. Neurosurg. 21, 360–368.

Newsome, M.R., Scheibel, R.S., Hanten, J.V., Wang, Z.J., Chu, Z., Li, X., and Levin, H.S. (2007a). Brain activation during working memory after traumatic brain injury in children. Neurocase 13, 19–24.

Newsome, M.R., Scheibel, R.S., Steinberg, J.L., Troyanskaya, M., Sharma, R.G., Rauch, R.A., Li, X. and Levin, H.S. (2007b). Working memory brain activation following severe traumatic brain injury. Cortex 43, 59–81.

Ng, S.M., Mukherjee, P., Ghajar, J., Johnson, C., Kobler, R.A., Sarkar, R., Lee, H., Mendez, M., Zimmerman, R.D., Manley, G.T., and McCandless, B.K. (2008). Extent of microstructural white matter injury in postconcussive syndrome correlates with impaired cognitive reaction time: a 3T diffusion tensor imaging study of mild traumatic brain injury. AJNR Am. J. Neuroradiol. 29, 1287–1292.

Niogi, S.N., Mukherjee, P., Ghajar, J., Johnson, C., Kolster, R.A., Sarkar, R., Lee, H., Meeker, M., Zimmerman, R.D., Manley, G.T., and McCandless, B.K. (2008). Extent of microstructural white matter injury in postconcussive syndrome correlates with impaired cognitive reaction time: a 3T diffusion tensor imaging study of mild traumatic brain injury. AJNR Am. J. Neuroradiol. 29, 967–973.

Niogi, S.N., Mukherjee, P., Ghajar, J., Johnson, C.E., Kolster, R.A., Lee, H., Suh, M., Zimmerman, R.D., Manley, G.T., and McCandless, B.K. (2008). Structural dissociation of attentional control and memory in adults sustaining mild traumatic brain injury. Brain 131, 3209–3221.

Nolin, P., Stipdonk, B., Ouimet, B., Allaire, C., Lavallee, M., Abeare, C.A., Reid, I., and Dupuis, F. (2008). Psychometric validation of the Paced Auditory Serial Addition Test (PASAT) in individuals with moderate to severe traumatic brain injury. Brain Inj. 22, 389–398.

Nolin, P., Stipdonk, B., Ouimet, B., Allaire, C., Lavallee, M., Abeare, C.A., Reid, I., and Dupuis, F. (2008). Psychometric validation of the Paced Auditory Serial Addition Test (PASAT) in individuals with moderate to severe traumatic brain injury. Brain Inj. 22, 389–398.

Nolin, P., Stipdonk, B., Ouimet, B., Allaire, C., Lavallee, M., Abeare, C.A., Reid, I., and Dupuis, F. (2008). Psychometric validation of the Paced Auditory Serial Addition Test (PASAT) in individuals with moderate to severe traumatic brain injury. Brain Inj. 22, 389–398.

Diffusion Tensor MR Imaging in Diffuse Axonal Injury

Konstantinos Arfanakis, Vicent M. Haughton, John D. Carew, Baxter P. Rogers, Robert J. Dempsey, and M. Elizabeth Meyerand

BACKGROUND AND PURPOSE: Disruption of the cytoskeletal network and axonal membranes characterizes diffuse axonal injury (DAI) in the first few hours after traumatic brain injury. Histologic abnormalities seen in DAI hypothetically decrease the diffusion along axons and increase the diffusion in directions perpendicular to them. DAI therefore is hypothetically associated in the short term with increased diffusion anisotropy. We tested this hypothesis by measuring the diffusion characteristics of traumatized brain tissue with use of diffusion tensor MR imaging.

METHODS: Five patients with mild traumatic brain injuries and 10 control subjects were studied with CT, conventional MR imaging, and diffusion tensor imaging. All patients were examined within 24 hours of injury. In each participant, diffusion tensor indices from homologous normal-appearing white matter regions of both hemispheres were compared. These indices were also compared between homologous regions of each patient and the control group. In two patients, diffusion tensor images from the immediate posttrauma period were compared with those at 1 month follow-up.

RESULTS: Patients displayed significant reduction of diffusion anisotropy in several regions compared with the homologous ones in the contralateral hemisphere. Such differences were not observed in the control subjects. Significant reduction of diffusion anisotropy was also detected when diffusion tensor results from the patients were compared with those of the controls. This reduction was also less evident 1 month after injury.

CONCLUSION: White matter regions with reduced anisotropy are detected in the first 24 hours after traumatic brain injury. Therefore, diffusion tensor imaging may be a powerful technique for in vivo detection of DAI.

Traumatic brain injury is a major public health problem, with about 2 million new cases reported in the United States each year (1). Most of these cases are classified as mild. However, approximately 30% of patients with the mild form experience some degree of residual neurologic or cognitive deficit (2). Common symptoms include deficit in attention, working memory, and speed of information processing, headache, dizziness, and irritability. Diffuse axonal injury (DAI) is widely believed to account for these persistent problems (3–5).

Experimental studies have demonstrated that diffuse white matter injuries may occur with traumatic brain injury irrespective of skull deformation (6). The mechanism for DAI is clear-strain deformation, a change in shape of the brain without a change in volume. Pathology studies have shown that DAI is characterized by multifocal lesions, scattered in white matter, that are occasionally associated with petechial hemorrhage (7). The three areas most commonly involved in DAI are the subcortical white matter, corpus callosum, and dorsolateral aspect of the upper brain stem. From a histologic aspect, several investigators (8–12) have linked DAI to focal misalignments of the cytoskeletal network or to changes of the axolemmal permeability, depending on the severity of the injury. In humans with mild traumatic brain injury, the first evidence of DAI is believed to be focal neurofilament misalignment, which becomes striking within the first 6 hours after injury (Fig 1) (8–11). This misalignment leads to an impairment of axoplasmic transport and focal accumulation of organelles. The effort continues for several hours after injury, causing focal swelling and expansion of the axonal cylinder (Fig 1). Over time, lysolution of the focal axonal swelling takes place, followed by disconnection of the axon at 30–60 hours after injury. After disconnection, the proximal and distal segments of the axon become sealed by a continuous axolemma and encompassed by an independent myelin sheath. A study using the tracer horseradish peroxidase determined that axolemmal permeability is not altered after mild traumatic brain injury (11). In moderate and severe traumatic brain injury, however, a change in the axolemmal permeability is the first evidence of injury. After several hours, the neurofilaments become misaligned, leading to focal swelling and disconnection (8, 11). Similar findings of focal axoplasmic impairment and swelling have been obtained in several different models of traumatic brain injury (13–15). The only disparity has been that in animals the same events occur much faster than in humans (9). In the most severe form of traumatic brain injury, in addition to the above-mentioned, direct severing of the axolemma may also occur (8).

Although the widely used Glasgow Coma Scale has excellent interobserver reliability and correlation with outcome following severe brain injury (16), it fails to differentiate between different types of injury with different prognoses and fails to localize the injury. CT or especially MR imaging, however, successfully demonstrates intracranial hematomas, subdural fluid collections, subarachnoid bleedings, cerebral edemas, and degenerating neurons (2, 17–21). Sufficient evidence exists that DAI is not a phenomenon secondary to edema, but occurs as a primary response to the traumatic brain injury. Therefore, none of these techniques are appropriate imaging tools for DAI.

A more recent noninvasive imaging technique, diffusion tensor imaging, as implemented in MR imaging (23, 24), can be used to probe, in vivo, the intrinsic diffusion properties of deep tissues. Diffusion tensor imaging has been applied in several studies to infer the microstructural characteristics of the brain (25, 26), the heart (27), and the spinal cord (28). In addition, diffusion tensor imaging has been introduced in the diagnosis of diseases conditions such as cerebral ischemia (29), acute stroke (30), and multiple sclerosis (31). Unlike conventional diffusion-weighted imaging (32), where diffusion-weighted images are used to calculate the scalar apparent diffusion coefficient, diffusion tensor imaging characterizes diffusive transport of water by an effective diffusion tensor **D**. The eigenvalues of **D** are the three principal diffusivities, and the eigenvectors define the local fiber tract direction field (23). Moreover, one can derive from **D** rotationally invariant scalar quantities that describe the intrinsic diffusion properties of the tissue. The most commonly used are the trace of the tensor (23, 25, 33), which measures mean diffusivity, and fractional anisotropy (FA) and lattice index (LI) (25, 33–35), which characterize the anisotropy of the fiber structure, meaning how much higher the diffusivity is along some directions compared with others.

The purpose of the study was to test the hypothesis that the histologic effects of DAI may be directly detected by means of diffusion tensor imaging in the first hours after injury, through a reduction of the axonal diffusion anisotropy. More specifically, we tested the possibility of using diffusion tensor imaging to detect DAI in patients with traumatic brain injury, by studying white matter regions that appeared normal on CT and other MR images, including apparent diffusion coefficient maps. We compared diffusion tensor imaging results between contralateral homologous structures of each subject and also between homologous structures of each patient and the control group. Finally, in the same normal-appearing white matter regions, we compared diffusion tensor imaging results in the first 24 hours after injury and in a follow-up study 30 days later.

Methods

Participants

This study included five patients with mild traumatic brain injury (three men and two women) and 10 volunteers with no known neurologic disorders (five men and five women). The mean age for the group of patients was 35.8 years (SD = 14.1 years), and for the control group 28.9 years (SD = 7.6 years). All patients were examined and studied as soon after admission to the emergency department as possible, but no later than 24 hours. Inclusion criteria for the study were a history of recent head trauma that caused the patient to exhibit acceleration or deceleration symptoms such as amnesia, disorientation, or confusion; a Glasgow Coma Scale score between 13 and 15; and the presence of a relative who could provide informed consent for the study. Exclusion criteria were evidence of large intracerebral hematomas, surgical hematomas, or hemicraniectomy, an indication for immediate surgical treatment of the head injury or other injury, an inability to cooperate with the

Received June 5, 2001; accepted after revision October 31.

From the Departments of Medical Physics (K.A., B.P.R., M.E.M.), Radiology (V.M.H.), Statistics (J.D.C.), and Biostatistics (R.J.D.), University of Wisconsin, Madison.

Address reprint requests to Konstantinos Arfanakis, 1111 University of Wisconsin–1500 Medical Sciences Center, 1300 University Ave., Madison, WI 53706-1532.

© American Society of Neuroradiology

...diffusion brain injury and relation to clinical outcome: a longitudinal study. Brain 131, 559–572.

Sidaros, A., Skimminge, A., Liptrot, M.G., Sidaros, K., Engberg, A.W., Herning, M., Paulson, O.B., Jernigan, T.L., and Rostrup, E. (2009). Long-term global and regional brain volume changes following severe traumatic brain injury: a longitudinal study with clinical correlates. Neuroimage 44, 1–8.

Sigmund, G.A., Tong, K.A., Nickerson, J.P., Wall, C.J., Oyoyo, U., and Ashwal, S. (2007). Multimodality comparison of neuroimaging in pediatric traumatic brain injury. Pediatr. Neurol. 36, 217–226.

Simoneau, A., Wortman, K., Muehlbeck, S., Mancer, F., Vallas, B., Tesiski, M., Kazanowska, I., Wahland, L.O., Soirdam, H., Leveleine, L., Ekner, A., and Sjoegren, C. (2011). The Axidiscribed transmissive for multi-centre MRI assessment of Alzheimer's disease: experience from the first 24 months. Int. J. Geriatr. Psychiatry 26, 75–82.

Sinson, G., Bagley, L.J., Cecil, K.M., Torchia, M., McGowan, J.C., Lenkowski, R.E., Mcintosh, T.K., and Grossman, R.I. (2001). Magnetization transfer imaging and proton MR spectroscopy in the evaluation of axonal injury: correlation with clinical outcome after traumatic brain injury. Am. J. Neuroradiol. 22, 143–151.

Sotela, A., Nakashima, T., Okumura, A., Kiwata, K., Shinda, J., and Iwama, T. (2005). Cognitive impairment after traumatic brain injury: a functional magnetic resonance imaging study using the Stroop Color-Word Test. Neurol. Regen. Sci. 29, Suppl. 3, 299–306.

Soustiel, J.F., Mahamid, E., Goldsher, D., and Zaaroor, M. (2008). Perfusion CT for early assessment of traumatic cerebral commotio. Neuroradiology 50, 189–196.

Sparos, G.K., Wilde, E.A., Bigler, E.D., Chevrinjer, H.B., Imzing, M.A., Levin, H.S., Li, X., and Hunter, J.V. (2007). Cerebellar atrophy after moderate-to-severe pediatric traumatic brain injury. Am. J. Neuroradiol. 28, 537–542.

Stanganar, G.E., O'Neil-Pirozzi, T.M., Goldstein, R., Kelkar, K., Kats, D.I., Burke, D., Rauch, S.L., Savage, C.R., and Glenn, M.B. (2008). Functional neuroimaging and cognitive rehabilitation for people with traumatic brain injury. Am. J. Phys. Med. Rehabil. 84, 62–75.

Suskauer, S.J., and Huisman, T.A. (2009). Neuroimaging in pediatric traumatic brain injury: current and future predictors of functional outcome. Dev. Disabil. Res. Rev. 15, 117–125.

Tang, L., Ge, Y., Sodickson, D.K., Miles, L., Zhou, Y., Reaume, J., and Grossman, R.I. (2011). Thalamic microstructure and connectome disruption in patients with mild traumatic brain injury. Radiology 260, 831–840.

Thornton, V.A., Hicks, R., Glasson, T., Miller, A.C., Sindhu, N., Crimon, J., and Schaub, K. (2010). Advancing integrated research in psychological health and traumatic brain injury: common data elements Arch. Phys. Med. Rehabil. 91, 1655–1656.

Tosoulidis, P., Carlsmurs, G.A., Di Paola, M., Pinzoles, M., Fera, F., Bonnere, R., Formisano, R., Pasqualetti, P., and Caltagirone, C. (2004). Gross morphology and morphometric asymmetries of the hippocampus, fornix, and corpus callosum of patients with severe noncontusive traumatic brain injury without macroscopically detectable lesions: a TI weighted MRI study. J. Neurol. Neurosurg. Psychiatry 75, 1316–1322.

Tsuchiya, D., Pirotsch, A., Bonilla, M., Cohen, A., Friedlander, A., and Shefel, I. (2011). Blood-brain barrier breakdown following traumatic brain injury: a possible role in posttraumatic epilepsy. Cardiovasc. Psychiatry Neurol. [Epub ahead of print]

Tong, K.A., Ashwal, S., Holshouser, B.A., Nickerson, J.P., Wall, C.J., Shutter, L.A., Osterdock, R.J., Haacke, E.M., and Kido, D. (2004). Diffuse axonal injury in children: clinical correlation with hemorrhagic lesions. Ann. Neurol. 56, 36–50.

Tong, K.A., Ashwal, S., Holshouser, B.A., Shutter, L.A., Herigstad, G., Haacke, E.M., and Kido, D.K. (2003). Hemorrhagic shearing lesions in children and adolescents with posttraumatic diffuse axonal injury: improved detection and initial results. Radiology 227, 332–339.

Trivedi, M.A., Ward, M.A., Hess, T.M., Gale, S.D., Dempsey, R.J., Rowley, H.A., and Johnson, S.C. (2007). Longitudinal changes in global brain volume between 79 and 409 days after traumatic brain injury: relationships with duration of coma. J. Neurotrauma 24, 756–777.

Tshibanda, L., Vanhaudenhuyse, A., Galanaud, D., Boly, M., Laureys, S., and Puybasset, L. (2009). Magnetic resonance spectroscopy and diffusion tensor imaging in coma survivors: promises and pitfalls. Prog. Brain Res. 177, 265–279.

Van Boven, R., Hamrington, G., Hackney, D., Ilvel, A., Grugio, C., Brunner, J., D'Esposito, M., Deste, J., Hauck, E., Isch, C., Jr., Jagust, W., Le Bihan, D., Mathis, C., Mueller, S., Mukherjee, P., Schuff, N., Chen, A., and Weiner, M. (2009). Advances in neuroimaging of traumatic brain injury and posttraumatic stress disorder. J. Rehabil. Res. Dev. 46, 717–737.

Vanvoordall, T.D., Cassella, N.C., Rao, V., Pointon, C.D., Gordon, B., and Schreiber, D.J. (2010). A morphometric analysis of neurosurgical lesions in traumatic brain injury. J. Neuropsychiatry Clin. Neurosci. 22, 173–181.

Warner, M.A., Marquez de la Plata, C., Spence, J., Wang, J.Y., Harper, C., Moore, C., Devous, M., and Diaz-Arrastia, R. (2010a). Assessing spatial relationships between axonal integrity, regional brain volumes, and neuropsychological outcomes after traumatic axonal injury. J. Neurotrauma 27, 2121–2130.

Warner, M.A., Youn, T.S., Davis, T., Chandra, A., Marquez de la Plata, C., Moore, C., Harper, C., Madden, C.J., Spence, J., McColl, R., Devous, M., Kang, R.D., and Diaz-Arrastia, R. (2010b). Regionally selective atrophy after traumatic axonal injury. Arch. Neurol. 67, 1336–1344.

Weinhall, E.M. (1996). Simple measurement of axonal stability for functional MRI imaging of activation in the brain. Magn. Reson. Med. 36, 643–645.

Wilde, E.A., Bigler, E.D., Gazella, P.V., Lowry, C.M., Bletz, D.D., Brooks, J., and Ryser, D.K. (2004). Alcohol abuse and traumatic brain injury: quantitative magnetic resonance imaging and neuropsychological outcome. J. Neurotrauma 21, 127–141.

Wilde, E.A., Bigler, E.D., Hunter, J.V., Fearing, M.A., Scheibel, R.S., Newsome, M.R., Johnson, J.L., Bachevalier, J., Li, X., and Levin, H.S. (2007). Hippocampus, amygdala, and basal ganglia morphometrics in children after moderate-to-severe traumatic brain injury. Dev. Med. Child Neurol. 49, 294–299.

Wilde, E.A., Bigler, E.D., Pedroza, C., and Ryser, D.K. (2009a). Post-traumatic amnesia predicts hippocampal volume in traumatic brain injury. Brain Inj. 23, 695–699.

Wilde, E.A., Chu, Z., Bigler, E.D., Hunter, J.V., Fearing, M.A., Hanten, G., Newsome, M.R., Scheibel, R.S., Li, X., and Levin,

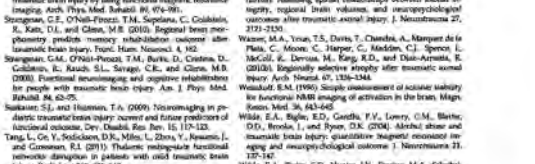

FIG 1. Illustration of the changes that axons undergo owing to cytoskeletal perturbation from mild traumatic brain injury.

A, The top neuron is healthy. In the bottom neuron, neurofilaments and, generally, cytoskeletal misalignment is shown a short time after injury. This impairs axonal transport.

B, Organelles accumulate in the injured region, causing the axon to swell locally and subsequently disconnect from the rest. In this Figure, the dimensions of the axons relative to the interaxonal space do not necessarily correspond to reality.

examination; and dental devices or other causes for degraded echo planar MR images or a contraindication for MR examination. All participants or the legal guardian signed an informed consent form in accordance with institutional policy.

Image Acquisition

CT scans were obtained in all patients. MR images were acquired in all patients and control subjects with use of a clinical 1.5-T imager with high-speed gradients (40 mT/m maximum amplitude, 150 mT/m/msec slew rate). The following conventional MR sequences were performed during each imaging session: 2D sagittal T1-weighted spin-echo localizer (600/ 8/1 [TR/TE/excitations], 90° flip angle, 24 × 24-cm field of view [FOV], 256 × 256 imaging matrix, 20 sections, 5-mm section thickness with 1.5-mm skip); 2D axial T2-weighted multiplanar prepared gradient-recalled acquisition in the steady state (600/ 25/1, 30° flip angle, 22 × 22-cm FOV, 256 × 256 imaging matrix, 23 sections, 5-mm section thickness with 2-mm skip); and 2D axial T1-weighted spin-echo (500/8/1, 90° flip angle, 24 × 24-cm FOV, 256 × 256 imaging matrix, 20 sections, 5-mm section thickness with 1.5-mm skip). Diffusion tensor imaging was performed with a modified 2D spin-echo sequence, with an echo planar imaging acquisition window and a pair of diffusion gradients symmetrically positioned around the 180° radio-frequency pulse. The imaging parameters were 4500/71.8/1, 24 × 24-cm FOV, 21 contiguous sections, 5-mm section thickness. The amplitude of the total diffusion gradient was 40 mT/m and was applied in 23 noncoplanar directions uniformly distributed in 3D space. The duration of each diffusion-weighted gradient lobe was 21.3 ms, and their temporal spacing was 26.9 ms. The effective diffusion weighting was $b = 100$ s/mm^2 (23). To estimate the diffusion tensor for all voxels, T2-weighted images with no diffusion weighting ($b = 0$ s/mm^2) (24) were also acquired at the beginning of each diffusion tensor imaging study. Echo planar readout was performed with a 128 × 128 image matrix, and all images were reconstructed to a 256 × 256 matrix after zero filling. Therefore, the resultant voxel dimensions were 0.9375 × 0.9375 × 5 mm^3. All diffusion tensor images ($b = 0$ s/mm^2 and $b = 1001$ s/mm^2) were acquired four times. The duration of diffusion tensor imaging was 7 minutes 12 seconds, and total imaging time for each subject was less than 15 minutes.

MR imaging and CT examinations were completed for all patients within the first 24 hours after injury. A second diffusion tensor imaging examination was performed in two of the patients 30 days after injury.

Postprocessing

All MR images were transferred to an offline workstation for postprocessing. The four repetitions of the images that were acquired with the diffusion tensor sequence were first averaged to increase the signal-to-noise ratio. Then, for the T2-weighted images with no diffusion weighting, a threshold was selected to remove CSF, and the averaged diffusion-weighted images were registered to these T2-weighted images to correct for distortions induced by eddy currents (36), by using a 2D perspective eight-parameter registration algorithm (37). Next, the diffusion tensor D and its eigenvalues and eigenvectors were estimated for all voxels (23). After sorting the eigenvalues in order of decreasing magnitude for each voxel, ($\lambda_1 > \lambda_2 > \lambda_3$), λ_1 represented the diffusivity along the primary diffusion direction ε_1 (23). In theory, the primary diffusion direction in a voxel coincides with the mean of the unit vectors that are parallel to the physical axes of the neurons included in that voxel. The second and third largest eigenvalues (λ_2, λ_3) represented the diffusivities along directions that were perpendicular to the primary diffusion direction, and to each other (23). The corresponding eigenvectors (ε_2, ε_3) represented those secondary diffusion axes. Several diffusion tensor imaging indices were also derived from the eigenvalues and eigenvectors in each voxel. One of these quantities is the trace of the diffusion tensor (23, 25, 33), which is a measure of the mean diffusivity. Diffusion anisotropy, which expresses the degree of selective diffusion along specific directions, was also measured, by means of FA and LI (25, 33–35). According to the definition of LI and FA, measurements of LI are characterized by a lower standard deviation than those of FA but are more susceptible to partial volume effects. Maps of trace, FA, and LI were constructed for all participants.

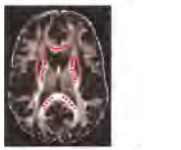

FIG 2. Example of the selection of voxels from the five structures under study, in one section of a control subject. The background image is an LI map. The red dots correspond to the selected voxels. The dots were made larger than the in-plane dimensions of a single voxel for visualization purposes.

A series of voxels was selected approximately in the left and right sides of the external capsule, posterior corpus callosum, anterior corpus callosum, posterior limb of the internal capsule, and anterior limb of the internal capsule in all subjects (Fig 2). For the patients with traumatic brain injury, these voxels were always selected from white matter that appeared normal on conventional MR images, even on brain maps. The selection was performed based on LI maps where the structures were easily identified. Since it was not trivial to detect the border between the posterior and the anterior limbs of the internal capsule based only on LI maps, where the two structures appear to be continuous, structure value color maps (38) were also produced for all subjects (Fig 3). In these maps, different colors represent specific directions in 3D space, and the intensity at each voxel is weighted by its LI value. The difference between the orientation of neurons in the posterior and the anterior limb of the internal capsule is such that the corresponding colors are significantly different, therefore simplifying the selection of the voxels (Fig 3). The same rules of voxel selection were applied to all patients and neurologically normal volunteers.

Each side (left, right) of the five abovementioned structures was considered as a supreme region of interest (ROI). Fifteen noncontiguous voxels were selected from each ROI. A total of 150 voxels (15 voxels × 5 structures × 2 hemispheres) were chosen in each participant. The selection was performed according to the following protocol. Since this sections (3 mm) were used for diffusion tensor imaging, portions of each ROI appeared in more than three sections. After identifying all the sections that contained each ROI, voxels from the three central ones were selected. In each one of these three sections, five noncontiguous voxels were selected per ROI. The voxels were evenly spaced from each other within the same section and ROI (Fig 2). Mean λ_1, λ_2, λ_3, trace, FA, and LI and their standard deviations were calculated for each ROI in both hemispheres in all participants.

The diffusion tensor imaging results from each structure in one hemisphere of the brain were compared with those from the contralateral hemisphere for all participants. In addition, the diffusion tensor imaging indices from each patient's ROIs were compared with those of the control group. The significance of any differences was assessed based on the assumption that the results from the control group were normally distributed. For all structures, values of diffusion tensor indices from the patients were indicated on graphs of the corresponding normal probability densities of the control group. Comparisons were also performed between the results from immediate (<1 day after injury) and short-term follow-up (30 days after injury) diffusion tensor images for two of the patients. For each selected structure, the side with the lower anisotropy on the immediate image was determined. Ratios of several diffusion characteristics between the ROIs with low anisotropy on the immediate image and their homologous contralateral ROIs with higher anisotropy were plotted for the immediate and follow-up data sets. A Student's *t* test was used to determine the statistical significance of the differences between hemispheres and between the immediate and follow-up data sets. A *P* value less than .05 was considered to indicate a statistically significant difference.

Results

For all patients, CT images exhibited no abnormalities. Conventional MR images, especially T2-weighted, and diffusion-weighted images and trace maps demonstrated scattered areas of abnormal signal intensity consistent with petechial hemorrhage or edema. In addition, for all patients, images of diffusion anisotropy (FA, LI) obtained with diffusion tensor imaging revealed regions of reduced anisotropy, differing from the hemorrhagic and edematous lesions (Fig. 4). These regions did not appear to be abnormal on the other types of images. However, anisotropy maps did not often provide sufficient contrast for detection of hemorrhages and edema, where anisotropy values might be similar to those in CSF or gray matter.

Interhemispheric comparisons of diffusion characteristics from the five selected structures in all neurologically normal control subjects showed no significant differences in anisotropy (Table). In two control subjects, a part of a selected structure in one hemisphere was characterized by a trace significantly higher ($P < .005$) than the trace of the homologous contralateral region. In all patients, significant differences ($P < .005$) were detected between the mean anisotropy of voxels selected from the two contralateral sides of several structures. The regions with reduced anisotropy were always characterized by a decrease in λ_1 and an increase in λ_2 and λ_3. However, in approximately 95% of the interhemispheric comparisons that were performed in the selected structures of the patients, and that resulted in significantly different anisotropy between the two sides, no significant differences in the trace were detected.

In many of the selected ROIs in each patient, anisotropy was significantly decreased with respect to the mean anisotropy in homologous ROIs in the control group ($P < .05$). No significant differences were observed between the trace values from homologous ROIs of each patient and the controls. However, ROIs with reduced anisotropy, compared with that in the control group, also exhibited reduced λ_1 and increased λ_2 and λ_3. Plotting the diffusion tensor imaging results for the patients on graphs of the corresponding distributions for the control subjects clearly demonstrated these observations (Fig 5). Significant reduction of anisotropy was more often detected in the internal capsule and corpus callosum and less often in the external capsule of the patients with mild traumatic brain injury.

Comparison of diffusion tensor imaging results obtained within 1 day and at 30 days after injury in two patients revealed significant changes in anisotropy in seven ROIs of both patients. In these ROIs, anisotropy values that were found to be lower than normal in the first data set were increased in the second. The corresponding trace values did not change between acquisitions, whereas λ_1 increased and λ_2 and λ_3 decreased. Plots of ratios of the diffusion characteristics between these seven ROIs and their homologous contralateral ones, in the immediate and follow-up data

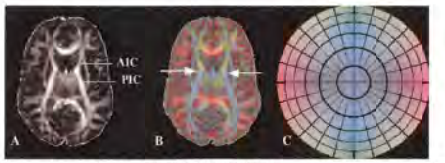

FIG 3. *A*, LI map in a control subject. The border between the anterior (AIC) and posterior (PIC) limbs of the internal capsule is not obvious from this image.

B, Absolute value color map of this same section as in *A*. Arrows indicate the exact level of the border between AIC and PIC. Color-representation of directions in 3D space helps to clearly separate the two structures.

C, Color circle demonstrates the correspondence of colors and directions in 3D space. This circle should be thought of as a 3D sphere that is viewed from below.

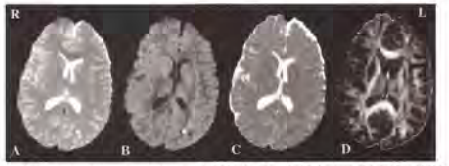

FIG 4. *A*, T2-weighted image in a patient with mild traumatic brain injury. Small hemorrhagic lesions are visible in the left occipital lobe and right frontal lobe.

B, Diffusion-weighted map of the same section in the same patient, for one of the 23 diffusion-weighted gradient directions. The abnormal regions from *A* are also visible in *B*.

C, Corresponding trace map. The same lesions from *A* and *B* can be detected.

D, LI map of the same section in the same patient. Decreased anisotropy is visible in the left internal capsule and left anterior corpus callosum. No abnormality was demonstrated in these regions with any other type of imaging. On this LI map, however, the hemorrhagic lesions from *A*, *B*, and *C* are hard to identify. *R* indicates right; *L*, left.

Diffusion characteristics of five structures from both hemispheres in a patient with mild traumatic brain injury and a healthy control subject

Structure and Parameter	Patient			Control Subject		
	Left Hemisphere	Right Hemisphere	*P* Value	Left Hemisphere	Right Hemisphere	*P* Value
Anterior corpus callosum						
λ_1	1.30 ± 0.15	1.69 ± 0.23	<0.0001	1.84 ± 0.17	1.88 ± 0.21	<0.6
λ_2	0.67 ± 0.17	0.45 ± 0.11	<0.0001	0.42 ± 0.12	0.43 ± 0.09	<0.6
λ_3	0.37 ± 0.11	0.29 ± 0.08	<0.0020	0.26 ± 0.07	0.27 ± 0.07	<0.5
Trace	2.34 ± 0.21	2.53 ± 0.23	>1	2.66 ± 0.21	2.72 ± 0.23	<0.5
FA	0.6 ± 0.08	0.76 ± 0.09	<0.005	0.80 ± 0.08	0.81 ± 0.06	<0.4
LI	0.47 ± 0.10	0.65 ± 0.1	<0.005	0.72 ± 0.11	0.73 ± 0.07	<1
Posterior corpus callosum						
λ_1	1.39 ± 0.27	1.64 ± 0.22	<0.2	1.73 ± 0.13	1.62 ± 0.16	<0.05
λ_2	0.47 ± 0.15	0.49 ± 0.12	<0.6	0.47 ± 0.10	0.49 ± 0.11	<0.6
λ_3	0.27 ± 0.09	0.34 ± 0.07	<0.2	0.23 ± 0.08	0.16 ± 0.09	<0.025
Trace	2.48 ± 0.25	2.56 ± 0.19	<0.3	2.41 ± 0.13	2.28 ± 0.19	<0.005
FA	0.72 ± 0.1	0.74 ± 0.09	<0.6	0.77 ± 0.05	0.79 ± 0.07	<0.3
LI	0.63 ± 0.12	0.65 ± 0.09	<1	0.69 ± 0.09	0.76 ± 0.06	<0.4
External capsule						
λ_1	1.29 ± 0.15	1.53 ± 0.15	<0.004	1.58 ± 0.13	1.55 ± 0.11	<0.5
λ_2	0.69 ± 0.15	0.53 ± 0.15	<0.1	0.61 ± 0.11	0.66 ± 0.08	<0.4
λ_3	0.37 ± 0.14	0.30 ± 0.11	<0.005	0.34 ± 0.11	0.37 ± 0.05	<0.2
Trace	2.34 ± 0.14	2.36 ± 0.16	<0.4	2.26 ± 0.19	2.28 ± 0.12	<0.4
FA	0.55 ± 0.15	0.69 ± 0.12	<0.005	0.58 ± 0.08	0.52 ± 0.06	<0.2
LI	0.59 ± 0.08	0.26 ± 0.05	<0.005	0.61 ± 0.09	0.57 ± 0.06	<0.1
Posterior internal capsule						
λ_1	1.23 ± 0.17	1.58 ± 0.15	<0.1	1.62 ± 0.11	1.61 ± 0.12	<0.5
λ_2	0.64 ± 0.07	0.54 ± 0.11	<0.005	0.49 ± 0.08	0.46 ± 0.07	<0.2
λ_3	0.36 ± 0.08	0.31 ± 0.09	<0.07	0.27 ± 0.06	0.24 ± 0.07	<0.4
Trace	2.24 ± 0.17	2.14 ± 0.15	<0.005	2.16 ± 0.09	2.12 ± 0.15	<0.2
FA	0.51 ± 0.09	0.62 ± 0.08	<0.005	0.70 ± 0.06	0.71 ± 0.07	<0.4
LI	0.41 ± 0.06	0.86 ± 0.08	<0.005	0.59 ± 0.06	0.60 ± 0.07	<0.4
Anterior internal capsule						
λ_1	1.24 ± 0.13	1.47 ± 0.06	<0.005	1.48 ± 0.15	1.55 ± 0.23	<0.025
λ_2	0.59 ± 0.05	0.52 ± 0.05	<0.01	0.56 ± 0.10	0.53 ± 0.10	<0.2
λ_3	0.42 ± 0.05	0.31 ± 0.04	<0.005	0.35 ± 0.09	0.33 ± 0.08	<0.3
Trace	2.25 ± 0.13	2.29 ± 0.12	<0.2	2.28 ± 0.24	2.41 ± 0.29	<0.1
FA	0.53 ± 0.09	0.68 ± 0.05	<0.005	0.63 ± 0.05	0.67 ± 0.09	<0.1
LI	0.38 ± 0.06	0.86 ± 0.04	<0.005	0.51 ± 0.06	0.53 ± 0.05	<0.1

Note.—Data are the mean ± SD. The values of λ_1, λ_2, λ_3, and trace were multiplied by 10^3 before they were included in the table and are in mm^2/s.

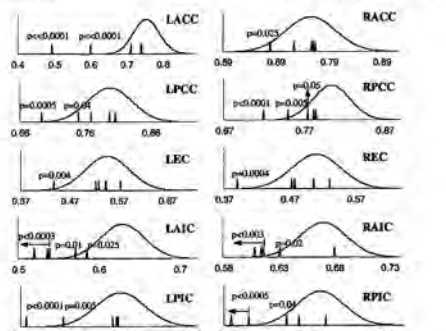

FIG 5. Graphs show distributions of FA results from 10 selected ROIs (5 structures × 2 hemispheres) for the control subjects (continuous lines) combined with the corresponding FA values for the five patients with mild traumatic brain trauma (vertical lines), in the left (*A*) and right (*B*) hemispheres. All horizontal axes represent FA values. *P* values are reported only for cases in which FA results for the patients were significantly different ($P < .05$) from the mean FA values of the control subjects. For the patients, anisotropy was found to be significantly reduced in several structures compared with normal values. Reduction of FA was more often in the internal capsule and corpus callosum and less often in the external capsule of the patients. *LACC* and *RACC*, indicate left and right anterior corpus callosum, respectively; *LPCC* and *RPCC*, left and right posterior corpus callosum; *LEC* and *REC*, left and right external capsule; *LAIC* and *RAIC*, left and right anterior internal capsule; *LPIC* and *RPIC*, left and right posterior internal capsule.

sets, demonstrated the temporal nature of the effects of mild traumatic brain injury on white matter (Fig 6). However, although the diffusion properties of these seven ROIs on the second image were more similar to normal, three of them were still characterized by anisotropy values and signal-to-noise ratios that were significantly different than normal, and four had reached "normal" diffusion characteristics ($P > .05$). In two ROIs with reduced anisotropy on the first diffusion tensor dataset, no significant change was observed 30 days later.

Discussion

Identification of DAI has been possible after death with invasive histopathologic studies. Electron microscopy, light microscopy, and immunocytochemical methods have been applied in excised human or animal, brain samples after traumatic brain injury in order to visualize DAI (39, 9, 40). MR imaging, with its ability to differentiate between various types of brain tissue in healthy or diseased conditions, has provided useful information about regions with lesions, such as edema and hemorrhage, following traumatic brain injury. However, conventional MR imaging underestimates the extent of DAI, which may account for much of the transient clinical pathologic conditions following traumatic brain injury and perhaps for the residual neurologic and cognitive deficits that are associated with traumatic brain injury. In this study, we tested the hypothesis that a relatively new MR imaging technique, diffusion tensor imaging, could be more effective in identifying the effects of DAI in vivo.

Images of FA and LI, as well as quantitative comparison of the diffusion characteristics of selected groups of voxels, demonstrated significant differences of diffusion anisotropy between the two sides (left, right) of several white matter structures in the patients. The same was not true in the neurologically normal control subjects. Therefore, regions with reduced anisotropy, compared with their contralateral homologous regions, may be possible sites of DAI. Although similar changes of anisotropy could be caused by edema or hemorrhage, there was no indication for the presence of such lesions on any CT or MR image. Furthermore, diffusivity values were not altered in the same regions. These results support the hypothesis that DAI may be detected by means of reductions in diffusion anisotropy. They may also explain why conventional diffusion-weighted imaging studies have not effectively detected DAI by using only measures of mean diffusivity (21).

In the patients, several regions were characterized by significantly lower diffusion anisotropy compared with the mean values from the control group. There was no indication for the presence of edema or hemorrhage in these regions. Although for several structures anisotropy values were abnormal, trace or mean diffusivity was not significantly different than the corresponding mean values for the control group. This observation also confirmed that our choice to study patients with mild traumatic brain injury by means of diffusion anisotropy instead of mean diffusivity was advantageous.

To understand how DAI may cause changes in the diffusion anisotropy values of white matter, one has to carefully study the results from histologic studies. Several researchers agree that the first indication of DAI in patients with mild traumatic brain injury is a misalignment of the cytoskeletal network (Fig 1A) (8–12). In addition, at low b values, similar to the ones used in our study, diffusion measurements are mostly sensitive to the extracranial space (41). Therefore, diffusion anisotropy in white matter is due to the fact that diffusion is more impeded perpendicularly to the fibers, mainly because of their geometric arrangement. In DAI, misalignment of the axonal membranes may increase restriction in diffusion parallel to the main axis of the neurons, thus decreasing λ_1. Additionally, misalignment of the cytoskeletal network may possibly increase diffusion in directions perpendicular to the axons due to an additional diffusion component, created by the projection of the primary diffusivity on the transverse plane, therefore increasing λ_2 and λ_3. Consequently, misalignment of the axonal membranes in DAI could be responsible for reductions of anisotropy. The second phase of DAI includes an impairment of axoplasmic transport and local accumulation of organelles, causing local swelling and expansion of the axonal cylinder (Fig 1*B*) (8–12). This change in shape may also increase restriction in the diffusion along the main axis of the fibers and decrease local diffusion anisotropy. Following lysis, disconnection may occur that might lead to the death of the distal and proximal segments of the neuron (8–12). The membrane of a dying neuron degenerates, thus reducing restriction in diffusion along directions perpendicular to the axon, increasing λ_2 and λ_3, and reducing anisotropy. For moderate and severe traumatic brain injuries, an increase of permeability also takes place in the injured axons (8–12). This may also increase diffusivity in directions perpendicular to the axons and reduce anisotropy. Some of the effects that can happen in DAI may not have occurred in the patients with mild traumatic brain injury in this study, either due to timing or due to severity of injury. However, all the possible histologic changes that have been associated with DAI may lead to a reduction in diffusion anisotropy through different mechanisms. Although we obtained no pathologic proof that the changes in diffusion anisotropy were associated with DAI, we could find no alternative plausible explanation.

A follow-up study in two patients with mild traumatic brain injury revealed that in some regions with initially reduced diffusion anisotropy the changes were partially, or completely, corrected 30 days after injury. These results should not be interpreted as evidence for regeneration of neurons. Instead, a cellular repair mechanism may have corrected the cytoskeletal misalignment and lobulation, before disconnection occurred. Thus, diffusion anisotropy increased at the axon returned to its original condition. In some cases, 30 days after injury, diffusion anisotropy was no longer different than normal values. This might be due to a complete repair process. In others, diffusion anisotropy was somewhat increased, but still significantly lower than normal. This could be explained with a repair process that was either not completed 30 days after injury, or it was finished and the final position of the axons was different than their healthy state. Finally, several white matter regions with reduced diffusion anisotropy one day after injury did not exhibit any change 30 days later. In these cases, disconnection might have happened, and Wallerian degeneration of the injured neurons might have occurred.

In a recent study of diffusion tensor imaging in two patients examined 1 year after severe traumatic brain injury, reduced anisotropy was detected in the internal capsule in one of the patients (42). This was claimed to be due to loss of the parallel fiber arrangement of the white matter tracts. Although this observation seems to agree with our results, it was acquired at a much later time after severe injury and cannot be easily compared. The same study also reported multiple sites of increased diffusivity in white matter. These data were translated as an expansion of the extracellular space, caused by neuronal or glial cell loss. The fact that we did not observe any changes in mean diffusivity in our study could be due to insufficient time for completion of Wallerian degeneration, or due to minor neuronal loss in connection with the mild injuries (43). Furthermore, the characteristics of the rest of the processes that take place in DAI in patients with mild traumatic brain injury might be such that mean diffusivity would not be significantly affected.

Most of the abnormalities in diffusion anisotropy values were detected in the internal capsule and the corpus callosum in the five patients. These results are in accordance with histology research in traumatic brain injury, which has concluded that the three sites most commonly involved in DAI are the subcortical white matter, the corpus callosum, and the upper brain stem. We did not perform any measurements directly inside the upper brain stem, because additional imaging time would have been required to include this structure. However, many axons that come through that region also belong to the internal capsule. Therefore, it is possible that the changes we observed in the diffusion characteristics of the internal capsule may be related to damage in the upper brain stem.

One of the limitations of our study was that not all of the voxels in the white matter structures under investigation were used. Instead representative voxels were selected from each structure. Although the selection was performed carefully and with very well determined criteria, the process was time-consuming and the results might be somewhat biased. A solution to this problem would be implementation of a segmentation algorithm that would segregate several white matter structures. This would allow investigation of more brain regions than those studied here, and also all the voxels in each structure could be accounted for.

An additional limitation of our study is the relatively small number of neurologically normal control subjects that were included. If more control subjects were available, we could have performed age-matched comparisons between the diffusion characteristics of each patient and the corresponding control subgroup. This is important since diffusion anisotropy is inversely proportional to the age of the subject (44). However, our measurements are not significantly affected, since the age of most of our patients was very similar to the mean age of the control subjects. Also, for the patients whose age was much different than the mean for the control subjects, the reduction of anisotropy that may have occurred due to age is much less significant than the changes we observed (44).

For two of the patients, we performed diffusion tensor imaging within 1 day of injury and 30 days after injury. It would be extremely interesting to acquire multiple diffusion tensor imaging data sets at short time intervals starting the first hours after injury. Initially, this might provide useful information about the severity of injury and the sites of DAI. Then a detailed longitudinal study would reveal how DAI progresses in each patient. Finally, after enough experience has been gained, longitudinal DTI studies in multiple patients with traumatic brain injury might provide knowledge that would assist physicians in predicting future changes in white matter that are characterized by DAI. Possible treatments could also be tested.

Moderate and severe traumatic brain injuries demonstrate, in addition to the effects found in the mild form, an increase in the permeability of the axon's membranes (8–12). Although we predicted that such changes would increase diffusivity in directions perpendicular to the axon and decrease diffusion anisotropy, diffusion tensor imaging in such patients is necessary to confirm this hypothesis.

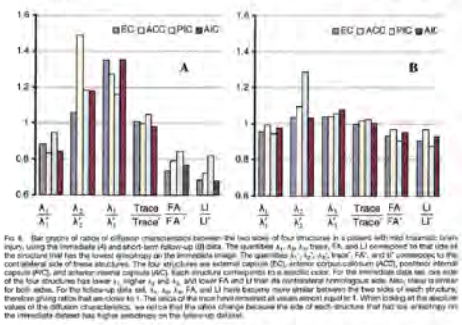

FIG 6. Bar graphs of ratios of diffusion characteristics between the two sides of four structures in a patient with mild traumatic brain injury, using the immediate (*A*) and short-term follow-up (*B*) data. The quantities λ_1, λ_2, λ_3, trace, FA, and LI correspond to that side of the structure that has the lowest anisotropy on the immediate image. The quantities λ_1', λ_2', λ_3', trace', FA', and LI' correspond to the contralateral side of these structures. The four structures are external capsule (EC), anterior corpus callosum (ACC), posterior internal capsule (PIC), and anterior internal capsule (AIC). Each structure corresponds to a specific color. For the immediate data set, the side of the four structures that have λ_1 higher or λ_2 and λ_3, and lower FA and LI than the contralateral homologous side. Also, trace is similar for both sides. For the follow-up data set, λ_1, λ_2, λ_3, FA, and LI have become more similar between the two sides of each structure, therefore giving ratios that are closer to 1. The ratios of the trace have remained at values almost equal to 1. When looking at the absolute values of the diffusion characteristics, we notice that the ratios change because the side of each structure that had low anisotropy on the immediate dataset has higher anisotropy on the follow-up dataset.

Conclusion

The present study demonstrated that DAI might be detected in patients with mild traumatic brain injury through a reduction of the diffusion anisotropy. Interhemispheric and intrahospect comparisons exhibited significant reduction of anisotropy in several white matter structures, early after injury. Most of the DAI sites appeared to be in the internal capsule and the corpus callosum. Furthermore, a follow-up study revealed several regions that might have recovered from the injury 1 month later. The technique presented herein might provide a tool for in vivo detection of DAI at the very early stages in patients with mild traumatic brain injury. This could have significant implications not only for the diagnosis but also for the treatment of these patients.

References

1. Gronwall D, Wrightson P. *The epidemiology of mild head injury.* In: Levin H, Eisenberg H, Benton A, eds. *Mild Head Injury.* Oxford: Oxford University Press, 1989:3–32
2. Miller RJ, Greenman RL, Hinds JP, et al. Prevalence of MR evidence of diffuse axonal injury in patients with mild head injury and normal head CT findings. *AJNR Am J Neuroradiol* 1994;15:1285–1289
3. Capruso DX, Levin HS. Cognitive impairment following closed head injury. *Neurol Clin* 1992;10:879–893
4. Evans RW. The postconcussion syndrome and the sequelae of mild head injury. *Neurol Clin* 1992;10:815–847
5. Levin HS, Mattis S, Ruff RM, et al. Neurobehavioral outcome following minor head injury: a three-center study. *J Neurosurg* 1987;66:234–243
6. Holbourn AHS. The mechanics of brain injuries. *Br Med Bull* 1943;3:147–149
7. Adams JH. Head Injury. In: Adams JH, Corsellis JAN, Duchen LW, eds. *Greenfield's Neuropathology.* 4th ed. New York: John Wiley and Sons, 1984:63–124
8. Povlishock JT, Christman JT. The pathobiology of traumatically induced axonal injury in animals and humans: a review of current thoughts. *J Neurotrauma* 1995;12:555–564
9. Christman CW, Grady MS, Walker SA, Holloway KL, Povlishock JT. Ultrastructural studies of diffuse axonal injury in humans. *J Neurotrauma* 1994;11:173–186
10. Grady MS, McLaughlin MR, Christman CW, Valadka AB, Fligner CL, Povlishock JT. The use of antibodies targeted against the neurofilament subunits for the detection of diffuse axonal injury in humans. *J Neuropathol Exp Neurol* 1976;52:143–152
11. Pierce EH, Christman CW, Corbett MC, Povlishock JT. Traumatically induced axonal membrane perturbation: its relationship to immediately induced reactive axonal change. *J Neurotrauma* 1994; 11:307–322
12. Gennarelli TA. The pathobiology of traumatic brain injury. *Neurotraumatol* 1997;23–31
13. Gennarelli TA, Thibault LE, Tipperman R, et al. Axonal injury in the optic nerve: a model simulating diffuse axonal injury in the brain. *J Neurosurg* 1989;71:244–253
14. Maxwell WL, Kerrigan AM, Graham DI, Adams JH, Gennarelli TA. Fluorescence studies of myelinic ensheathment nerve fibers after diffuse axonal injury. *Acta Neuropathol* 1989;78:195–400
15. Tomei G, Spagnoli D, Cherici A, Monaco S. Morphology and neurophysiology of fatal axonal injury experimentally induced in the guinea pig optic nerve. *Acta Neuropathol* 1990;80:590–610
16. Ong L, Sedzimir BM, Duchen MR, Adam M, Lee MS. The prognostic value of the Glasgow Coma Scale, hypoxia and computerized tomography in outcome prediction of pediatric head injury. *Pediatr Neurosurg* 1996;24:205–209
17. Kelly AB, Zimmerman RD, Snow RB, Grandy SL, Heier LA, Deck MDF. Head trauma: comparison of MR and CT—experience in 100 patients. *AJNR Am J Neuroradiol* 1988;9:699–708
18. Firlinger ED, Brooks WM, Jung RE, Hart BL, Yeo RA. Proton MR spectroscopic findings correspond to neuropsychological function in traumatic brain injury. *AJNR Am J Neuroradiol* 1998;19: 1879–1885
19. Hofman PAM, Stapert SZ, van Kroonenburgh MJPG, Jolles J, de Kruijk J, Wilmink JT. MR imaging, single-photon emission CT, and neurocognitive performance after mild traumatic brain injury. *AJNR Am J Neuroradiol* 2001;22:441–449
20. Hofman PAM, Kemerink GJ, Jolles J, Wilmink JT. Quantitative analysis of magnetization transfer images of the brain: effect of closed head injury, age and sex on white matter. *Magn Reson Med* 1999;42:803–806
21. Liu A, Maldjian J, Bagley L, Sinson G, Grossman R. Traumatic brain injury: diffusion weighted imaging findings. *AJNR Am J Neuroradiol* 1999;20:1636–1641
22. Adams JH, Graham DI, Murray LS, Scott G. Diffuse axonal injury due to nonmissile head injury in humans: an analysis of 45 cases. *Ann Neurol* 1982;12:557–563
23. Bauer PJ, Matlachov A, Le Blanc D. MR diffusion tensor spectroscopy and imaging. *Biophys J* 1994;66:259–267
24. Basser PJ, Mattiello J, Le Bihan D. Estimation of the effective self-diffusion tensor from the NMR spin echo. *J Magn Reson B* 1994;103:247–254
25. Pierpaoli C, Jezzard P, Basser PJ, Barnett A, Di Chiro G. Diffusion tensor MR imaging of the human brain. *Radiology* 1996;201:637–648
26. Virta A, Barnett A, Pierpaoli C. Visualizing and characterizing white matter fiber structure and architecture in the human pyramidal tract using diffusion tensor MRI. *Magn Reson Imaging* 1999; 17:1121–1133
27. Huisman AA, Sorlien DY, Winston KL. Direct histological validation of diffusion tensor MRI in formaldehyde-fixed myencephalon. *Magn Reson Med* 2000;44:157–161
28. Pierpaoli DA, Narayana PA. In vivo diffusion tensor imaging of rat spinal cord with echo planar imaging. *Magn Reson Med* 1999;42: 366–306
29. Lythgoe MF, Sinar AL, Calamante F, et al. Effects of diffusion anisotropy on lesion delineation in a rat model of cerebral ischemia. *Magn Reson Med* 1997;38:662–666
30. Van Gelderen P, de Vleeschouwer MHM, DesPres D, Pekar J, van Zijl PCM, Moonen CTW. Water diffusion and acute stroke. *Magn Reson Med* 1994;31:154–163
31. Wozniak DF, Clark CA, Barlow GJ, Thompson AJ, Miller DH. Diffusion tensor imaging of studies and gerbil-spanning white matter in multiple sclerosis. *Neurology* 1999;52:1626–1632
32. Le Bihan D. Diffusion NMR imaging. *Magn Reson Q* 1991;7:1–30
33. Basser PJ. Inferring microstructural features and the physiological state of tissues from diffusion-weighted images. *NMR in Biomed* 1995;8:333–344
34. Basser PJ, Pierpaoli C. Microstructural and physiological features of tissues elucidated by quantitative-diffusion-tensor MRI. *J Magn Reson B* 1996;111:209–219
35. Pierpaoli C, Basser PJ. Toward a quantitative assessment of diffusion anisotropy. *Magn Reson Med* 1996;36:893–906
36. Henriques JC, Moore JB. Correction for distortion of echo-planar images used to calculate the apparent diffusion coefficient. *Magn Reson Med* 1995;34:960–964
37. Woods RP, Dapretto ST, Holmes CJ, Cherry SR, Mazziotta JC. Automated image registration. II. geometric validity and global accuracy, intermodality validation. *J Comp Assist Tomogr* 1998;22:141–154
38. Pierotti S, Pierpaoli C. Color schemes to represent the information of anisotropic tissues from diffusion tensor data: application to white matter fiber tract mapping in the human brain. *Magn Reson Med* 1997;42:52–62
39. Adams JH. Head Injury. In: Adams JH, Duchen LW, eds. *Greenfield's Neuropathology.* 5th ed. Edward Arnold, 1992:488–452
40. Gentleman SM, Nash MJ, Sweeting CJ, Graham DI, Roberts GW. β-amyloid precursor protein (βAPP) as a marker for axonal injury after head injury [letter]. *Lancet* 1993;160:190–146
41. Le Bihan D, Mangin JF, Poupon C, et al. Diffusion tensor imaging: concepts and applications. *J Magn Reson Imaging* 2001;13:534–546
42. Bigg-Gunn HJ, Symon MR, Barker GJ, Greenwood R, Ebmeier IS. Diffusion imaging shows abnormalities after blunt head trauma when conventional magnetic resonance imaging is normal. *J Neurol Neurosurg Psychiatry* 2002;76:830–833
43. Gennarelli TA, Thibault LE, Adams JH, Graham DI, Thompson CJ, Marcyniuk RP. Diffuse axonal injury and traumatic coma in the primate. *Ann Neurol* 1982;12:564–574
44. Parchelmann A, Sullivan EV, Hedehus M, Lim KO, Adalsteinsson E, Moseley M. Age-related decline in brain white matter anisotropy measured with spatially corrected echo-planar diffusion tensor imaging. *Magn Reson Med* 2000;44:259–268

NIH Public Access
Author Manuscript

Published in final edited form as:
J Clin Exp Neuropsychol. 2011 June; 33(6): 638–647. doi:10.1080/13803395.2010.537223.

An fMRI Investigation of Episodic Memory after TBI

Kathryn C. Russell[1,2], Patricia M. Arenth[1,2], Joelle M. Scanlon[1], Lauren J. Kessler[1], and Joseph H. Ricker[1,2]

[1] University of Pittsburgh Department of Physical Medicine and Rehabilitation

[2] University of Pittsburgh Center for the Neural Basis of Cognition

Abstract

Traumatic brain injury often negatively impacts episodic memory; however studies of the neural substrates of this impairment have been limited. In this study, both encoding and recognition of visually presented stimuli were examined with functional magnetic resonance imaging. Twelve adults with chronic complicated mild, moderate, and severe injuries were compared with a matched group of twelve controls. Behavioral task performance did not differentiate the groups. During neuroimaging, however, the group of individuals with traumatic brain injury exhibited increased activation, as well as increased bilaterality and dispersion as compared to controls. Findings are discussed in terms of increased resource recruitment.

Traumatic brain injury (TBI) is defined as an injury to the brain incurred through externally inflicted trauma. Such injuries may result in significant impairment of an individual's physical, cognitive and psychosocial functioning. One specific type of cognitive ability known to be compromised after TBI is episodic memory (Hanninen, Perhiin, Isoniemi, Helmiss, & Kurki, 2006; Levin et al., 1990; Millis & Ricker, 1994; Sieker, et al., 2010; Wagner & Deuders, 1999; Wright, Schmitter-Edgecombe & Woo, 2010). As classically defined (e.g., by Baddeley, Harris, Sunderland, Watts & Wilson, 1987), the term episodic memory describes the ability to recall information regarding previously experienced stimuli, or events linked to a specific point in time. While the term "episodic memory" encompasses several types of cognitive tasks and operations, in the clinical setting episodic memory is most frequently assessed by having individuals learn a stimulus set for recall and/or recognition at a later point in time.

While it may be argued that other persisting cognitive deficits after TBI may cause even greater functional disablement than episodic memory (i.e., executive control deficits), individuals with TBI have been shown to have significant awareness of memory difficulties (Anderson & Schmitter-Edgecombe, 2009). In addition, assistance with memory issues has been one of the most frequently cited needs of individuals at one year post injury (e.g., Corrigan, Whiteneck, & Mellick, 2004). This awareness of need may be due to the fact that episodic memory difficulties can have a significant impact on daily living; in day to day functioning, impairment in episodic memory may contribute to difficulties with learning and retaining new information, as well as recall of functional tasks, appointments, assignments, and obligations. While such difficulties may range from mild to severe, it is important to note that the diffuse and complex nature of TBI may result in multiple areas of cognitive deficit, with additive effects. As a result, even mild episodic memory impairment, when combined with executive control and other cognitive difficulties, may potentially have a significant impact on the ability of an individual to complete household tasks or function at most employment settings.

There have been numerous behavioral studies of episodic memory impairment following TBI (e.g., Blanchet, Paradis-Giroux, Pepin, & McKerral, 2009; Deshpande, Millis, Rendec, Fuerst, & Ricker, 1996; Millis & Ricker, 1994; Tsaira et al., 2010; Wagner & Donders, 1999). Taken together, these have clarified the nature of such deficits after injury (emphasizing the multifactorial nature of impairment in the acquisition of novel information, rather than solely a failure in retrieval). Although these contributions to the literature have been significant, there has been surprisingly minimal exploration of the cerebral substrates of this type of cognitive difficulty.

Our capacity to characterize the cerebral correlates of cognitive function in both healthy and clinical populations has been greatly expanded with the development of functional neuroimaging technologies. In studying TBI, such methods provide unique opportunities for identifying the pathophysiology of cognitive dysfunction related to injury in areas such as episodic memory. In the first study to apply functional imaging technology to the examination of episodic memory in persons with TBI, Ricker and colleagues (2001) utilized oxygen-15 positron emission tomography (O-15 PET) to study a group of persons with severe TBI at 1 to 3 years post injury. In comparison to matched controls, persons with TBI displayed increased overall activation, as well as increased bilaterality in activation patterns during an episodic memory task, even when task performance was not significantly different. In addition, activation patterns were noted to be more diffuse and more posterior as compared to healthy individuals. The authors asserted that the increased blood flow, more widespread dispersion and altered lateralization found in the TBI groups may indicate that increased cognitive effort is required to complete the same cognitive task as healthy controls due to decreased cognitive efficiency associated with brain injury. In addition, they suggested that the more posterior activation may represent the employment of a different strategy for remembering, or differential processing of the stimuli. In a subsequent O-15 PET study of memory following TBI, Levine and colleagues (2002) demonstrated that although individuals with TBI did not perform significantly differently on particular behavioral memory tasks and did engage the frontal, temporal and parietal areas normally activated by the retrieval of verbal learning paradigms, they also displayed relative increases in activation of the frontal, anterior cingulate and occipital regions and decreased activation in the right dorsomedial thalamus. Overall, the authors concluded that the TBI participants displayed alterations in the functional neuroanatomical networks used by healthy controls for memory. They further concluded that this may represent neural reorganization due to injury-related disconnection.

Despite the differences in technologies, fMRI studies of memory have demonstrated similar findings to those reported above. It should be noted, however, that the majority of fMRI studies in persons with TBI have examined working memory, while the study of episodic memory in this population remains quite novel. In fact, in addition to the study presented here, our research of the literature revealed only two other fMRI studies of TBI which employed episodic memory paradigms. The first of these studies (Strangman et al., 2008) involved the teaching of a verbal learning strategy to a group of 54 individuals with documented memory impairment after TBI. fMRI scanning was then conducted during the encoding phase only of a verbal learning paradigm. After scanning, free recall and recognition for the word lists was tested. The aim of the study was to assess the efficacy of fMRI results at the baseline session to predict rehabilitation outcome after a subsequent 12 session rehabilitation program focused on teaching of internal strategies for memory improvement. The rehabilitation program was followed by 2 post-test sessions of neuropsychological testing, with no repeat fMRI. For primary and secondary fMRI analysis,

Address correspondence to: Kathryn C. Russell Laboratories of Cognitive Neuroscience, Department of Physical Medicine & Rehabilitation, 3471 Fifth Avenue, Suite 201, Fifth Avenue Place, Pittsburgh, PA 15213, U.S.A. krussell@pitt.edu

J Clin Exp Neuropsychol. Author manuscript; available in PMC 2012 June 1.

6 regions of interest (ROI) were selected for prediction analysis based on areas activated using the same learning paradigm with a matched group of healthy controls. The findings of this study supported the assertion that the left prefrontal areas, are related to strategic verbal learning, as these areas of activation were observed in the TBI group, as well as the control group. They also observed that BOTH under and overactivation in the TBI group was associated with reduced performance on memory tasks after rehabilitation, creating an inverted-U quadratic relationship between performance and activation, which was therefore predictive of outcome. The authors asserted that underactivation may represent structural injury to the gray or white matter within the region of interest or possibly injury to areas projecting to the region, while overactivation may indicate tissue and engaged cortical areas, which, despite, "effortful utilization", failed to produce improvement in functional memory as tested.

Strangman and colleagues (2009) conducted an additional study of 20 participants with TBI and 20 healthy controls using the same behavioral and fMRI paradigm as the 2008 study. The aims of this study were to evaluate whether individuals with TBI and controls activated the same networks during verbal learning, and whether TBI affected neural activity during encoding when participants were instructed to use semantic clustering. Despite baseline testing indicating significant differences in behavioral performance between groups, direct comparison of group fMRI activation across all tasks, indicated no significant differences, suggesting that individuals in the TBI group activated the same general networks as healthy controls. Additional analysis and modeling focused on regions of interest (ROIs) with known anatomical connectivity which had been identified as being differentially activated by both groups during semantic (directed) strategy encoding. These comparisons indicated decreased activity for individuals with TBI in these key ROI's, as compared to controls. The authors postulated that these decreases may be reflective of the decreased behavioral performance by the TBI group, or may indicate the use of different networks or strategies by the TBI group during this specific type of encoding. Further functional connectivity analysis which suggested a functional (bi) rat anteriorical breakdown in connectivity between the left DLPFC and other areas normally associated with strategic control.

Together, these studies indicate significant alterations in functional cerebral processing of memory following TBI, as has been shown in previous PET studies. It is relevant to note that fMRI working memory studies have also shown that, relative to healthy controls, persons with TBI demonstrate alterations in hemodynamic response in terms of both blood flow and dispersion of cortical activation associated with working memory tasks conducted during fMRI. This has been found with individuals with moderate to severe injury (Chen, Mukherjee, et al., 2001; Perlstein, et al., 2004) as well as with individuals with mild TBI (Chen, et al., 2004; McAllister et al., 1999, 2001). In addition, other studies conducted using different working memory load conditions have shown altered patterns of activation between groups, and have suggested differential recruitment of cortical areas for individuals with TBI as compared to controls (Newsome et al., 2007, Turner & Levine 2008).

Given the relative novelty of neuroimaging studies of episodic memory following TBI, the goal of the present study was to add significantly to the literature in this critical area through further characterization of the cerebral activation during episodic memory task performance with fMRI. As alterations in cerebral activation have been noted for individuals with various levels of injury, even when behavioral performance was within functional limits, we included individuals with complicated mild, moderate, and severe levels of TBI, along with a healthy control group. For group comparison, each participant completed neuropsychological testing of cognition, as well as both encoding and recognition phases of an episodic memory task within an fMRI scanner. Given previous findings using O-15PET and fMRI during memory tasks, it was anticipated that alterations in activation, dispersion,

and laterality would be observed in the current study for the group with TBI as compared to the control group. Because of our expectations that differences in activation patterns for participants with TBI may occur outside of those activated by healthy controls, we chose not to follow an ROI approach as used by Strangman et al (2008, 2009). Our assessment was that a voxel-based approach would allow an opportunity to capture and evaluate activation which may occur outside of regions prescribed by previous studies of healthy controls. In doing so, our aim was to gain additional information which may help to characterize the changes in neural functioning following TBI, as change may involve altered recruitment of networks and functional brain areas. As so few neuroimaging studies of episodic memory after TBI have been conducted, we felt that exploring these characteristics in a more holistic fashion was critical to providing a base for further neuroimaging studies of episodic memory after TBI.

In addition, it should be noted that prior memory studies have generally conducted fMRI during encoding or retrieval individually. In the present study we chose to examine activation patterns of both encoding and recognition within the same fMRI session. Based on the limited neuroimaging studies of individuals with TBI, and what is known from studies of healthy individuals, we hypothesized that individuals with TBI would demonstrate greater cerebral activation as well as differential dispersion of activation during both encoding and recognition.

In addition we felt that it was important to document whether or not these alterations would in fact be observed, and also to begin to describe differences based on memory process. No other study has made this comparison in individuals with TBI.

Method

Participants

Participating in this study were 15 persons with TBI and 14 uninjured controls. Because of technical difficulties and/or subject movement, the data from some fMRI sessions were not usable. Thus, included in the current paper are 12 controls (2 F) and the 12 persons with TBI (3 F) with usable fMRI data. All participants were right hand dominant and were free of any history of neurological disease or insult (excepting the traumatic brain injury for the injury group), psychiatric illness, and alcohol or drug abuse. No participant met any of the standard exclusionary criteria for MRI, including metal in the body or pregnancy. All participants gave consent approved by the Institutional Review Board of the University of Pittsburgh.

We included TBI participants with moderate and severe, as well as complicated mild initial traumatic brain injury based on history confirmed by medical record data. Classification of moderate to severe injury was made based on the lowest Glasgow Coma Scale (GCS; Teasdale & Jennett, 1974) score in the first 24 hours after injury (moderate defined as GCS of 9 – 12 and severe defined as GCS of 3–8, as well as objective medical documentation indicating TBI. Those with mild initial injuries (i.e., GCS ≥ 13) were only included if there was sufficient documentation of significant medical complications following injury, such as positive neuroradiologic findings. Those persons with "complicated mild" injuries were included, as research has shown that such persons have outcomes more similar to those of persons with moderate TBI (Kashluba, Hanks, Casey, & Millis, 2008; Williams, Levin, & Eisenberg, 1990). Initial GCS scores in our study group ran the full range from 3–15 (M = 8.9, SD = 5.5), with best GCS scores in the first 24 hours ranging from 7–15 (M = 12.2, SD = 3.4). These scores suggest that, on average, persons in the TBI group sustained relatively severe injuries. Due to hemodynamic alterations that are associated with acuity rather than cognitive activation in the first several months after injury (Yamaki, et al., 1996) TBI participants were at least one year post-injury, but not greater than 3 years post-injury (M = 1.7 years, SD = 0.6 years, range = 1.06–2.61 years). Though inclusion for the TBI participants was originally determined through medical records and prior scans, structural scans collected for this study were examined. The majority of the residual findings seen on the T2 structural scans were diffuse. Residual focal lesions in the TBI group were few, and there was no consistent trend towards any contusion location (1 bifrontal, 1 right temporal, 1 basal ganglia). Control scans all appeared to be age-appropriate and within normal limits.

Controls were matched to the TBI group for age, gender, and number of years of education. Age matching was achieved through age stratification with five-year strata. Within each age stratum, participants were matched for educational level within one year. The groups included in this paper were not significantly different in age (controls: M = 26.5, SD = 8.7, range = 19–50; TBI: M = 33.1, SD = 12.9, range = 18–54; t(22) = -1.46, p = 0.16), or number of years of education (controls: M = 16.2, SD =2.8, range = 12–22; TBI: M = 14.8, SD = 1.9, range = 12–18; t(22) = 1.37, p = 0.19). Complete participant demographics for the TBI group are presented in Table 1.

Materials and Design

During the imaging session, four pairs of stimulus blocks were presented. For each pair, the first was an encoding block and the second was a recognition block. The four types of stimuli used were black line drawings (pictures), black outline shape arrays (shapes), black capitalized words (words), and black capitalized non-pronounceable letter strings (letters). All were displayed on a white background. The pictures were from Snodgrass & Vanderwart (1980), the words were developed from their original set (as used by Noble, Johnson, & D'Esposito, 1998; Raye, Johnson, Mitchell, Nolde, & D'Esposito, 2000), and both words and pictures were high-frequency, easily named and visualized items. Shape stimuli were unfamiliar abstract arrays composed of primary shapes, and letter stimuli were unpronounceable 4–8 letter strings. During encoding blocks, participants were shown sets of items of one of the four stimulus types, and for each item made a yes/no pleasantness judgment (e.g., McDermott, et al., 1999) for the purpose of enhancing attention and encoding. During each block, only one type of stimulus was presented, and each block contained approximately 6-minute run for the fMRI session. During recognition blocks, stimulus sets consisted of half previously seen items and half new items. Participants were asked to identify if a presented item had been previously seen or not by pressing one of two buttons on a response pad. While the recognition block for a particular stimulus type was presented immediately following the corresponding encoding block, the ordering of the four pairs of blocks was counterbalanced among participants. Items within each block were randomly ordered. When considering the eight functional scans together with the structural scans, each scanning session totaled around 1 hour and 15 minutes.

E-prime software (www.pstnet.com) was used for stimulus presentation. Trials were set up so that following a 500 msec fixation cross, an item was presented for 2500 msec. The stimulus screen was followed by a blank screen presented for 1000, 3000, or 5000 msec.

Procedure

After informed consent was obtained, the questionnaires and neuropsychological assessments were completed. The Token Test (DeRenzi & Vignolo, 1962; Spreen & Benton, 1969) was given in order to ensure participants could understand and follow verbal instructions. An estimate of overall intelligence was obtained using the Wechsler Test of Adult Reading (WTAR; Wechsler, 2001). Although TBI and control group members were matched, as previously described, by age and education level, the average WTAR standard score for the TBI group fell in the average range (mean = 101, SD = 9.2), while the average WTAR standard score for the Control Group fell in the high average range (mean = 116, SD